



OPEN ACCESS

EDITED BY

Sonu Gandhi,
National Institute of Animal Biotechnology
(NIAB), India

REVIEWED BY

Avtar Singh,
Molekule Inc., United States
Ajeet Kaushik,
Florida Polytechnic University, United States

*CORRESPONDENCE

Ahmed Noah Badr,
✉ an.badr@nrc.sci.eg
Khaloud Mohamed Alarjani,
✉ kalarjani@ksu.edu.sa

RECEIVED 18 February 2024

ACCEPTED 09 July 2024

PUBLISHED 31 July 2024

CITATION

Alarjani KM, Yehia HM, Badr AN, Ali HS,
Al-Masoud AH, Alhaqbani SM, Alkhatib SA,
Rady AM and Abdel-Maksoud M (2024),
Antimicrobial impact of a propolis/PVA/
chitosan composite and its prospective
application against methicillin resistance
bacterial infection.
Front. Nanotechnol. 6:1387933.
doi: 10.3389/fnano.2024.1387933

COPYRIGHT

© 2024 Alarjani, Yehia, Badr, Ali, Al-Masoud,
Alhaqbani, Alkhatib, Rady and Abdel-Maksoud.
This is an open-access article distributed under
the terms of the [Creative Commons Attribution
License \(CC BY\)](https://creativecommons.org/licenses/by/4.0/). The use, distribution or
reproduction in other forums is permitted,
provided the original author(s) and the
copyright owner(s) are credited and that the
original publication in this journal is cited, in
accordance with accepted academic practice.
No use, distribution or reproduction is
permitted which does not comply with these
terms.

Antimicrobial impact of a propolis/PVA/chitosan composite and its prospective application against methicillin resistance bacterial infection

Khaloud Mohamed Alarjani^{1*}, Hany Mohamed Yehia²,
Ahmed Noah Badr^{3*}, Hatem S. Ali⁴, Abdulrahman H. Al-Masoud²,
Sarah M. Alhaqbani¹, Shahad A. Alkhatib¹, Ahmed M. Rady¹ and
Mostafa Abdel-Maksoud¹

¹Department of Botany and Microbiology, College of Science, King Saud University, Riyadh, Saudi Arabia, ²Food Science and Nutrition Department, College of Food and Agricultural Sciences, King Saud University, Riyadh, Saudi Arabia, ³Food Toxicology and Contaminants Department, National Research Centre, Cairo, Egypt, ⁴Food Technology Department, National Research Centre, Cairo, Egypt

Seriously damaged skin could be infected by methicillin-resistant bacteria, which delays restoration. Propolis has bioactivity linked with its minor components, such as antimicrobials and antioxidants. Active sites in polyvinyl alcohol (PVA) and chitosan (CS) can enhance the nano-loading of natural extracts with activity amelioration. Korean propolis extract (KPE) loading to a nanocomposite possibly enhances its antimicrobial and anti-inflammatory potency. Composites were formed using two PVA/CS structures (1:1; 2:1), and their skin-application appropriateness was determined by mechanical properties, moisture content, water activity, and color. The composite of PVA/CS (1:1) was more practicable for KPE-loading. Increasing KPE concentrations (50, 100, 150, and 200 ng/mL) alters composite bioactivity measured by Fourier transmission infrared (FT-IR). Antibacterial potency of 200 ng KPE/mL was the most effective concentration, followed by 150 ng KPE/mL, against *Staphylococcus aureus* (MRSA) and *Clostridium perfringens*. The composite activity was measured as minimum inhibition (MIC) and minimum bacterial concentrations (MBC). At 200 ng KPE/mL, MIC and MBC against MRSA were 14.93 ± 1.21 and 20.21 ± 1.97 mg composite/mL, respectively. Significant inhibition was also recorded for antibiofilm formation, where MRSA growth was not detected after 4 hours of time intervals to the stainless-steel coupon. Compared to planktonic bacteria, the formed barrier of PVA/CS restrained the biofilm matrix formation and supported KPE antimicrobial. The impact of inhibition against biofilm formation depends on two parallel mechanisms (PVA barrier with hydrogen bonds, besides nano-KPE particle penetration into bacterial cells). The KPE-composite application to rats' wounds shows significantly reduced MRSA infection. The results demonstrate the capability of KPE composite in reducing infection, healing correctly, and restoring hair. The wound swabbed test emphasizes this capacity, in which bacterial growth

rate restriction was evaluated using a plate count assay. The results recommended 150 ng KPE/mL loading into CS/PVA (1:1) as an effective anti-pathogenic treatment, particularly against the MRSA infection of wounds.

KEYWORDS

propolis antimicrobial activity, chitosan/PVA formulas, membrane characteristics, nanocomposites, skin infection, methicillin resistance *Staphylococcus aureus* (MRSA), *Clostridium perfringens*, wound healing

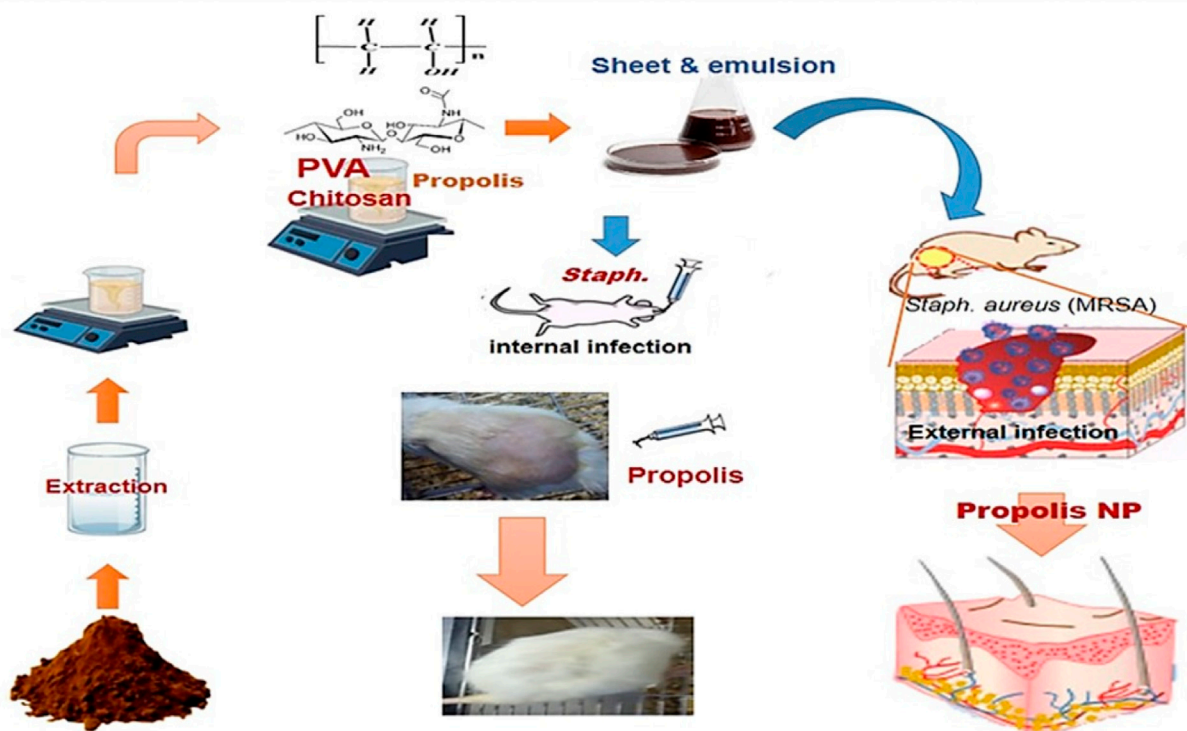
1 Introduction

Propolis is a resinous material bees produce from various botanical sources; its primary function is to seal and safeguard the beehive. Flavonoids and phenolic compounds are two types of antioxidants found in propolis, which are significant for fighting the harmful effects of free radicals and reducing oxidative stress (Kurek-Górecka et al., 2014; Saleh et al., 2023). Propolis has robust antibacterial capabilities, rendering it efficacious against many strains of bacteria, viruses, and fungi (Boisard et al., 2015; Pobiega et al., 2017; Salatino, 2022). The attribute stems from the origin of propolis used by bees, which serves to establish a sterile environment inside the hive and prevent illnesses. Propolis has an immune-modulatory action, regulating the immune system and effectively increasing its capacity to combat detrimental stimuli (El-Seedi et al., 2022). Propolis has the potential to mitigate inflammation inside the human body. This characteristic is

significant in wound healing and immune system regulation (Pascoal et al., 2014; Oryan et al., 2018; Zuhendri et al., 2022). Propolis can induce tissue regeneration and establish a defensive barrier against microbial infections. Dermatitis, eczema, and acne are inflammatory skin disorders affected by propolis applied directly to the skin area (Działo et al., 2016; Kim et al., 2019). This efficacy is linked with propolis' antibacterial activity (Oryan et al., 2018).

Staphylococcus aureus, a member of the Gram-positive bacteria family, presents a significant risk for many skin-related illnesses since it develops resistance to methicillin medications. The MRSA infection causes more danger than HIV/AIDS in United States hospitals due to its difficult-to-treat co-morbidities, ease of transmission, and higher fatality rate (Verma et al., 2021). Nevertheless, some antibiotics, like Vancomycin, daptomycin, linezolid, and clindamycin, retain their efficacy. Natural extracts are active against *Staphylococcus aureus* infection, less hazardous than chemical antibiotics, and safe for public health. Several studies

Antimicrobial Impact of a Propolis/PVA/Chitosan Composite and its Prospective Application against Methicillin Resistance Bacterial Infection



GRAPHICAL ABSTRACT

have shown that natural extracts can stop the growth and spread of methicillin-resistant *Staphylococcus aureus* (Maureen et al., 2019). Wound infection leads to several complications, particularly the contamination of methicillin-resistant bacteria. Successful wound management effectively reduces infections, which promotes prompt healing and minimizes pathological consequences (Boateng and Catanzano, 2015). *Staphylococcus aureus* and *Clostridium perfringens* were implicated in various wound infection disorders (Khandia et al., 2021). Besides, bacteria biofilm formation is a common factor contributing to impaired wound healing, resulting in a subsequent delay in the overall healing process. Hence, there is a significant need for an efficient treatment that controls skin wound infection and accelerates its recovery (Percival et al., 2012). Nanoparticles kill bacteria by breaking down cell membranes and blocking or changing enzyme pathways (Yah and Simate, 2015). The presence of PVA in propolis loading nanocomposite can enhance the antibacterial potency of the extract against Gram-positive and Gram-negative bacteria of human pathogens (Saleh et al., 2023). In this regard, the applicable formation of propolis may impact its efficacy.

Nanocomposite is an intelligent application aiding efficacy enhancement; it possesses pharmacological, antibacterial, or antioxidant properties regarding their bioactive constituent contents (Pisoschi et al., 2018; Singh et al., 2022). Composite formulation bases include gums, proteins, oligosaccharides, and specific lipids (Ribeiro et al., 2021; Zhang et al., 2021). Structuring nanocomposites with more than a polymer provides a mix of beneficial characteristics constructed from original components (Cai et al., 2016). Polyvinyl alcohol (PVA) and chitosan (CS) are used in nanoparticle formulation because of their emulsifying and stabilizing properties (Hu et al., 2017; Verma et al., 2022). Loading active ingredients, like propolis extract, into nanocomposites is vital in improving its biological effectiveness, control release, and deliverability (MaHam et al., 2009). Recent research has focused on investigating targeted nanotechnology systems with potential applications in wound healing (Naskar and Kim, 2020). Lately, there has been significant progress in nanoscale systems designed for drug administration (Singh et al., 2022). Nanoparticles can traverse cell membranes, while traditional antibacterial drugs often exhibit restricted permeability across specific cell membranes (Zou et al., 2020). PVA and CS have been widely studied and identified as promising materials for tissue engineering applications. Previous studies have shown the ability of PVA-chitosan complexed dressings to accelerate wound healing. For instance, nanofiber dressing containing PVA/CS as a core-shell reflected distinguished physical characteristics with antioxidant potency (Barzegar et al., 2021). Again, lignin/CS/PVA complexed hydrogels significantly enhanced wound healing in a rat wound model (Zhang et al., 2019). Meanwhile, loading cerium oxide NPs into PVA-chitosan hydrogel boosted significant antibacterial activity (Kalantari et al., 2020). Otherwise, linking the aromatic ring to the CS structure improves the antibacterial activity (Risha Achaiah et al., 2023). These aromatics can be gained from propolis extract due to its polyphenolic content. That complex formed due to hydrogen bonds in the CS or PVA with a phenolic ring of the KPE content may result in natural and active antibiotics against MRSA infection.

The current need is to create a new category of natural antibiotics that can effectively combat MRSA by using distinct

modes of action. This study aimed to utilize Korean propolis extract, characterized previously in our previous work (Alarjani et al., 2023), to apply for loading at nanocomposite (consisting of chitosan/polyvinyl alcohol), where CS dispersing in PVA solution. Hydrogen bonds formed due to the active groups on PVA and CS (-OH, NH₂, C-H) can assist in the KPE nanoemulsion characterization's loading activity, indicating the suitable formula and applications. The methicillin-resistant *Staphylococcus aureus* (MRSA) strain ATCC 33591 was applied to cause infection in rat wounds. An *In vivo* study evaluating the Korean propolis extract (KPE) nanocomposite mitigation impact on infected wounds was utilized to emphasize KPE-nanocomposite efficiency as a safe remedy for the inflammation and hair loss of rats exposed to MRSA infection. A swabbing assay for the bacterial count on the infected wounds was assessed using plate count media to emphasize the KPE-composite reduction effect.

2 Materials and methods

2.1 Chemicals and materials

Korean propolis powder was purchased from the Raydel Korea Mart, Gangnam-daero, Seocho-gu, Seoul, Republic of Korea. Chitosan powder with low Mw: 100,000 to 120,000 Da; deacetylate degree: 75%–85%; and polyvinyl alcohol (CAS No.:9002-89-5) with molecular weight (Mw): 98,000; polymerization degree: 2800; % hydrolysis mole: 99.0%–99.8% were the raw materials utilized for the wound film preparation (Merck, Chaoyang District, China).

Microbial media of tryptic soy broth (TSB, Millipore 105459), nutrient agar (NA; Millipore 105450), Mueller–Hinton (MA, Millipore 103872), reinforced *clostridium* medium broth (RCM, Millipore 91365), and mannitol salt agar (MSA, Millipore 105404) were utilized for the evaluation of antibacterial and antifungal activities. Each media was prepared according to the manufacturing methodology, and the application conditions were adjusted according to the applied assay. All chemicals, solvents, and media were purchased from Sigma-Aldrich Chemie GmbH[®], Eschenstr, Taufkirchen, Germany.

2.2 Microorganisms

The applied microorganisms were methicillin-resistant *Staphylococcus aureus* (MRSA) strain ATCC 33591 and *Clostridium perfringens* NCTC 8237, utilized for propolis composites estimation activity against the standard vancomycin antibiotic. The strain was taken as a gift from the Toxicology and Food Contaminants Department, National Research Centre, Cairo, Egypt. This isolate was grown on nutrient agar slants (38°C ± 2°C/16 h) and stored in a cooler (2°C) until usage. Before the evaluation, the test was reactivated using nutrient broth tubes (38°C ± 2°C/24 h).

2.3 Preparation of the propolis nanoemulsion and nanoparticles

For the extraction and application processes, the powder was ground to near micronized granules (20 mesh) and instantly dried

(40°C ± 2°C) in a hot-air oven (ED 56 Oven, Binder GmbH, Tuttlingen, Germany) till dried completely. Korean propolis extract (KPE) was prepared using the same methodology as the previous research (Alarjani et al., 2023).

The nanoemulsion solution was carried out using the following two steps. Firstly, 6 g of dried chitosan was prepared, added to 200 mL of acidic distilled water (1% lactic acid), and stirred (2 h/25°C); then sodium tri-poly-phosphate solution (0.4%, w/v) was added. Afterward, the formed suspension was stirred overnight (500 rpm; 22°C ± 3°C). By the time it ended, a glycerol-sorbitol mixture (2:1) was added at 35% (regarding chitosan weight) and then stirred (2 h). After the time was completed, several concentrations of KPE (0, 50, 100, 150, and 200 ppm) were individually added to a part of the formed solution. Each solution part was continuously stirred (30 min) till it reached complete harmony.

Parallel to that, a second solution of PVA was prepared (3 g/100 mL distilled water) using a clean beaker and was placed on a hotplate stirrer (model ARE 5, Velp, Via Stazione—Usmate Velate—Italy) to dissolve PVA powder (up to 6 h) completely. The formed PVA solution was added drop-wise to the solution parts of chitosan–propolis during their homogenization (Ultra-Turrax T25, IKA Janke & Kunkle, GmbH Co., Germany) at the conditions of 16,000 rpm/8 min/0°C, followed by ultrasonic probe treatment (Ultrasonic Homogenizers H, ultrasonic converter UW2070, booster horn, SH 213 G and microprobe tip MS 73, Ø 3 mm). The solution was poured into the composite-forming medium and placed in a hot-air oven (40°C/12 h) for sheet formation. It was kept in a dry condition for the subsequent evaluation. Two composites were formed using the previous solutions at 50%:50% (1 CS/1 PVA) and 25%:75% (1 CS/2 PVA), and the dry-formed films were evaluated for tensile stress values.

2.4 Determination of propolis film mechanical properties

The film tensile examination and elongation at break were evaluated using ASTM method D882-01 (Cao et al., 2007) with minor modifications. Evaluated samples (50 mm × 10 mm × 0.85 mm) were tensioned until the gap formed between the grasp heads of a texture analyzer (TAXT plus 50, Stable Micro Systems Ltd., Surrey, United Kingdom). The initial grip separation distance was 30 mm, and the crosshead speed was 100 mm/min. The elongation at break and tensile examination were calculated by dividing the final extension at rupture and maximum load by the cross-sectional area of the sheet, respectively.

2.5 Morphological investigation

A scanning electron microscope (Quanta Fei 450, United States; acceleration voltage 20 kV) was utilized to investigate the surface morphology of created prepared films. After cutting the samples into parts with dimensions of 5 mm by 5 mm, they were laid down on top of carbon tape; then, photographs of the sample were captured using a scanning electron microscope (SEM). The samples were first subjected to gold sputtering for a 3 min duration using an Edwards S 150 Sputter Coater, resulting in a coating with a thickness of 150 Å (Cárdenas et al., 2010).

2.6 Swelling behavior

A phosphate-buffered saline (PBS) solution was utilized to estimate the swelling behavior of the CS/PVA composite sheet. This step was performed by immersing the samples in the solution. The weight of the sample was determined to be accurate at particular time intervals ranging from 0 to 7 h. The sample's swelling (%) determination was calculated at each time interval, and a graph was drawn to show the relationship between the time interval and swelling percentage (Singh et al., 2016).

2.7 Moisture retention capacity

The moisture content of the prepared composite was evaluated as previously investigated (Kalia et al., 2021). After being prepared, the film samples were sliced into uniform sizes, and the starting weight of each sample was recorded as Wt1. The heat level inside the oven was regulated at 40°C the whole time. In the end, the weight of the teaching sample was determined and pointed out as Wt2. The equation that was utilized for estimating the capacity of moisture retention (MRC) is as follows:

$$\% \text{MRC} = \frac{Wt1}{Wt2} \times 100\%$$

Where, MRC: moisture retention capacity.

Wt1: initial weight of the composite sheet.

Wt2: final weight of the composite sheet.

2.8 Assessment of the color, thickness, and morphology characteristics

The prepared nanoemulsion's displayed color was examined using a Hunter LAB (Color Hunt XE, Hunter Lab, United States). The viewing angle was 10°, and the light source illuminated the D65. The L* (lightness), a* (negative = green, positive = red), and b* (negative = blue, positive = yellow) were the parameters employed to determine the color's value. Referenced gravimetric techniques were used to calculate the moisture content of the dried film samples. About 10 g of the film was dried in a hot air oven (at 103°C ± 2°C) until a constant weight was achieved (AOAC). The AQUALAB 4TE (NE Hopkins, Pullman, WA 99163, United States) was utilized to test the water activity of film samples (Sun et al., 2017). The thickness of the prepared dry sheets was measured at five different points to an accuracy of 0.001 mm using a 3M301A—STORM™ digital micrometer (STORM, Wellington Ave, Cranston, United States) (Otoni et al., 2014).

2.9 Thermogravimetric (TGA), X-ray diffraction, and Fourier transform infrared (FTIR) analyses

Thermogravimetric analysis was conducted on the PVA/CS-based composite using a simultaneous TGA thermal analyzer (SDT 2960, TA Instruments, United Kingdom). The experiments were performed with a heating rate of 10°C/min, up to 600°C, and keeping

a continuous air flow rate. The X-ray diffraction (XRD) analysis was performed using a Rigaku-Model Miniflex apparatus. The temperature range for the analysis was set from 2°C to 40°C, with a scanning rate of 0.05° per minute and a step size of 0.02°. The X-ray radiation was CuK α , with a precise wavelength of 1.542 Å.

Regarding the FTIR measurements, samples were cut into tiny discs with a 1 cm diameter. Fourier transforms infrared (FTIR) transmission spectra were collected on a Perkin-Elmer FTIR spectrophotometer in the 4,000–400 cm⁻¹ frequency range with a resolution of 4 cm⁻¹.

2.10 Minimum inhibitory concentration (MIC)

The microdilution assay determined the propolis nanocomposite's minimum inhibitory concentration (MIC) against *Staphylococcus aureus* and *C. perfringens* (Almeida et al., 2017). The KPE-loaded film was dissolved in dimethyl sulfoxide (DMSO). Using the 100 μ L MH media in 96-well microplates, an inoculation of MRSA bacteria (1.31×10^5 CFU/mL) was tested against applied KPE concentrations in DMSO at 0.625, 1.25, 2.5, 5.0, 10, 20, 40, 80 mg/mL media (Wiegand et al., 2008). The McFarland solution scale was applied to adjust the bacterial concentration, and a control negative (DMSO) and control positive (Zethromycin; standard antibiotic). The microplates were incubated (37°C \pm 1°C/24 h) using an anaerobic incubator chamber (AS-580, Anaerobe Systems Co, Morgan Hill, CA 95037, United States), supported with a gas system (5% CO₂, 5% H₂, 90% N₂). After the time was finished, a 30 μ L resazurin solution (100 μ g/mL) was injected into the wells where the MIC value defined as the lowest concentration inhibited bacterial growth. The MBC was calculated by inoculating 100 μ L aliquots from each well of the microplate and then testing the inhibition at the MIC level using Petri plates with tryptic soy–yeast extract broth. The MBC was calculated by inoculating 100 μ L aliquots from each well of the microplate, in which inhibition was evaluated for the MIC wells on Petri plates containing tryptic soy–yeast extract broth media and incubated (at 37°C/24 h). The minimum effective bactericidal concentration (MBC) was determined to be the lowest concentration at which 99.9% of the injected cells were first killed.

2.11 Assessment of propolis complex MRSA antibiofilm

Stainless steel coupons (type 304; 1 cm diameter) were cleaned, washed, and sanitized according to the methodology described before (Narayanan et al., 2016). Each stainless-steel coupon was submerged in a 24-well polystyrene microplate filled with 1.0 mL of inoculum (MRSA or *C. Perfringens*). The microplates were hermetically sealed using Parafilm[®], followed by a polystyrene cover of each plate before incubation (at 37°C/24 h) using an anaerobic incubator chamber (AS-580, Anaerobe Systems Co, Morgan Hill, CA 95037, the United States), supported with a gas system (5% CO₂, 5% H₂, 90% N₂). After

preparing the coupons, they were immersed in a CS/PVA complex with different propolis concentrations (50 ng, 100 ng, 150 ng, 200 ng/mL), where the inoculated coupon loaded with MRSA bacteria (1.31×10^5 CFU/mL) or *C. perfringens* (1.54×10^5 CFU/mL). The plates containing the coupon immersed in the nanoemulsion complex were shaken (300 rpm) using a microplate shaker during incubation (IKA MS 3, United States), which offers laminar flow conditions for the antibiofilm solution. The bacterial log of cell count was recorded for each hour of contact, up to 6 hours of experimental time. Reducing the bacterial count regarding propolis composite coating of coupons was determined against the control ones, which were infected by bacterial colonies without composite coating (Amalaradjou and Venkitanarayanan, 2014).

2.12 Propolis composite assessment against MRSA infection in rats

The *in vitro* models highlighted the propolis composite as more effective against the MRSA strain than *C. perfringens*. As an *in vivo* model, researchers utilized thirty male Sprague Dawley rats, each 3 months old and weighing 180.64 \pm 5.67 g. The rats were allowed to acclimate for 1 week in an acrylic tank while being kept in regular laboratory settings (standard laboratory animal diet and water were provided *ad libitum*, and the light/dark cycle lasted 12 h), and the rats were classified as follows:

Group 1: Rats with skin injuries had MRSA infection treated with propolis-free film.

Group 2: Rats with skin injuries had MRSA infection treated with Vancomycin (150 ng/mL).

Group 3: Rats with skin injuries had MRSA infections treated with propolis (50 ng/mL).

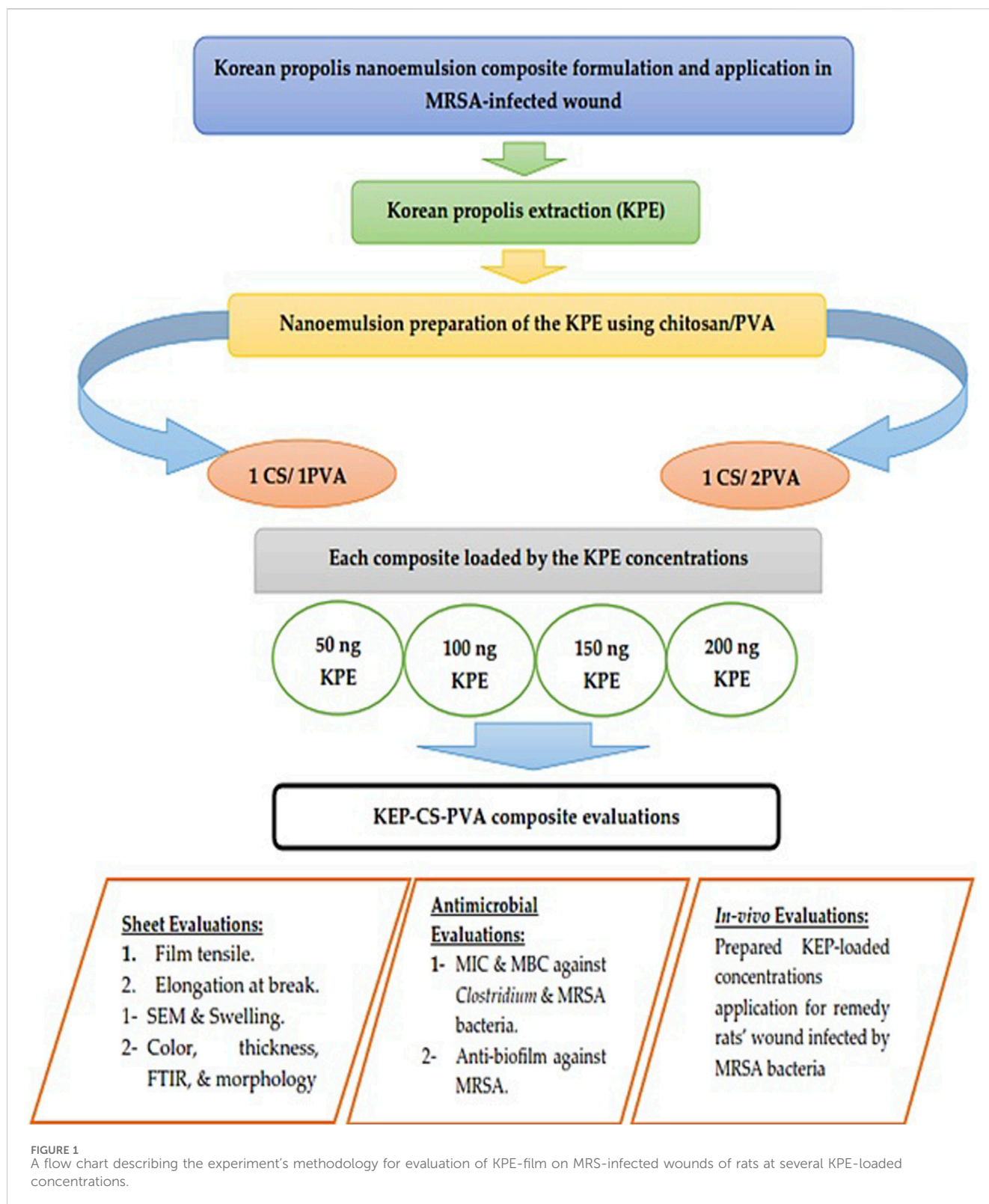
Group 4: Rats with skin injuries had MRSA infection treated with propolis (100 ng/mL).

Group 5: Rats with skin injuries had MRSA infections treated with propolis (150 ng/mL).

Group 6: Rats with skin injuries had MRSA infection treated with propolis (200 ng/mL).

The bacterial strain treated Rats in groups as chronic infection (MRSA bacteria inoculation at 1.31×10^5 CFU/mL). Rats' wounds were re-contaminated every 5 days at days (1, 5, and 10) before applying the remedy with a composite coating containing Korean propolis extract nanoparticles as an antimicrobial agent.

Ketamine (80 mg/kg), followed by xylazine (10 mg/kg), was injected intramuscularly into the femoral musculature of the hind leg for anesthesia (Grada et al., 2018; Bhatia et al., 2022). After loss of reflexes, the rat was placed in the prone position on the heating pad on an operating table. After that, a full-thickness wound was produced with a 6 mm punch tool in the right up legs of rats. After the wound production, the rat was placed in an induction chamber and subjected to an induction dose varying from 2% isoflurane to 100% oxygen at a rate of 1.5 L/min until loss of the reflexes. Rats for infection were treated using the MRSA bacterial solution at a concentration of 1.31×10^5 CFU/mL. For the treatment, rats were administrated twice daily by coating the injury (each 12 h) during the next



18 days; the response for curing was recorded daily. After propolis complex treatment, the microtiter plate assay for the MRSA bacterial cell was checked utilizing the viable plate count technique to determine the number of bacterial populations that had survived (Amalaradjou et al., 2010).

2.13 Data statistical analysis

The data were reported using means \pm standard deviations (SD; $n = 5$). Statistical analysis was performed using analysis of variance (ANOVA). The multiple range test conducted by Duncan was

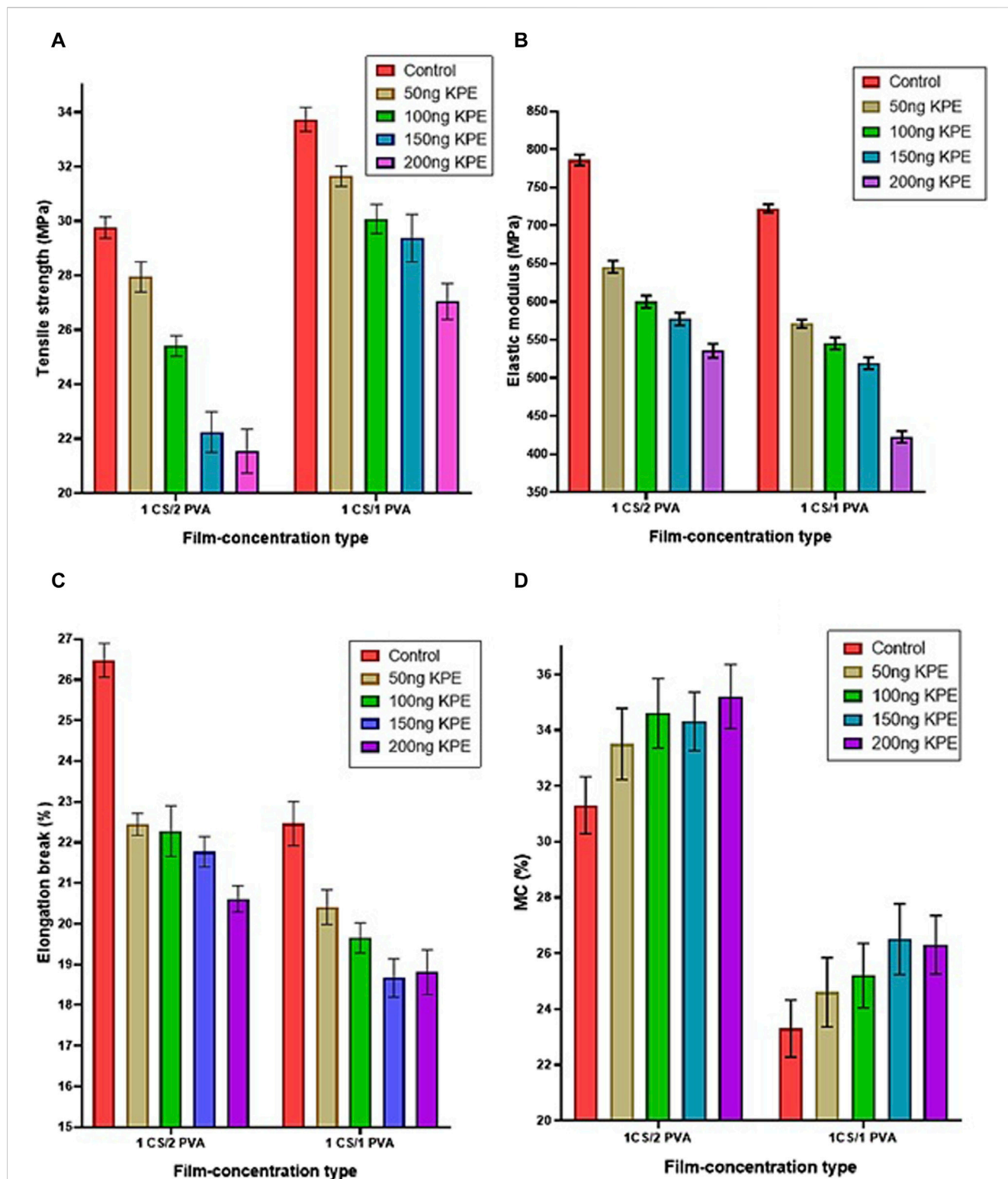


FIGURE 2 Mechanical characteristics and moisture content of two film composites with different propolis extract concentrations. (A) Representation of the changes in tensile stress values regarding the changes in film concentrations and propolis content. (B) Representation of the changes in elastic modulus values regarding the changes in film concentrations and propolis content. (C) Representation of the changes in the elongation at break values regarding the changes in film concentrations and propolis content. (D) Representation of the changes in moisture content values regarding film concentrations and propolis content changes. KPE, Korean propolis extract; CS, chitosan; PVA, polyvinyl alcohol; MC, moisture content.

calculated, and the difference between the mean values was considered significant (at $p \leq 0.05$).

3 Results

The KPE nanoparticle formed in light of the schematic diagram reflects a significant activity for both *In vitro* and *In vivo* assessment. The flow chart describing the experiment's methodology for evaluating KPE film on MRS-infected wounds of rats at several KPE-loaded concentrations illustrates the evaluation steps (Figure 1).

3.1 Composite mechanical, morphological, and moisture properties

The dried film properties of two composites (1 CS: 1 PVA and 1 CS: 2 PVA) are studied; results are the way to recommend a significant formula for the application. Tensile stress was measured with and without different amounts of propolis complex (50, 100, 150, and 200 ng/mL). According to the data in Figure 2A, the tensile stress values decreased by adding propolis to film structures. Lowering the tensile values reduced the film's flexibility and ability to withstand stress before breaking. It was also seen that adding propolis to the (1 CS: 2 PVA) film changed the tensile stress values more than in the case of the (1 CS: 1 PVA) composite, which may be linked to PVA concentration. The elastic modulus is, at its core, a measure of how strong a material is and how easily it can be bent or stretched (Figure 2B); this could support numerous applications of this composite. Again, adding propolis made the changes in the elastic modulus value stand out more in the (1 CS: 2 PVA) composite than in the (1 CS: 1 PVA) composite, where only minor changes were seen in the last film composite. Another parameter utilized for the film material assessment was the elongation at break (Figure 2C). This characteristic indicates the extension of the material that can be measured as stretching before the break occurs in its structure. All these properties support the utilization of the (1 CS: 1 PVA) composite formula as a more sustainable one.

Adding propolis to the films consisting of chitosan and polyvinyl alcohol materialized as a treatment causing elongation weakness, being implicated in an equal proportion (1 CS: 1 PVA) or a double PVA concentration (Figure 2C). Apparent changes were recorded for the elongation at the break values. It is worth mentioning that when applying different percentages of propolis, the changes recorded were more severe, with the film containing a higher PVA percentage. The insertion of propolis extract into the film material reflects an elevation of its moisture content (%MC). Again, the high PVA film recorded a higher moisture content than the lower PVA film (Figure 2D). However, the MC percentages were lower for all (1 CS: 1 PVA) films with different KPE concentrations than the film composite (1 CS: 2 PVA). The previous results indicate the extent to which composites containing various concentrations of Korean propolis extract excel in giving the properties of elasticity and softness, especially when loaded onto a 1 CS:1 PVA composite. However, the composites loaded with the same propolis concentrations at a 1CS:2 PVA composite had lower flexibility,

softness, and drying speed at the application site. All these results support the preliminary evidence of the superiority of the compound containing 1:1 in application in terms of cohesion, speed of drying, and effectiveness when applied to the skin. At this point, SEM was utilized to evaluate the 50, 100, 150, and 200 ng KPE/mL composite.

The morphological makeup of the formed composite is a significant factor for numerous practical applications of PVA/chitosan composites. Selected images for the SEM describing the surface of the PVA/CS composite were examined. Figure 3 shows the images chosen for the scanning electron microscope (SEM) that demonstrate the surface structure of PVA/CS composites (1:1) loading with KPE at several concentrations (50, 100, 150, and 200 ng/mL). The PVA/CS exhibited a uniform surface for all captures with several KPE concentrations. The captures also reflect the smoothability of the composite surface. It was noticed that large particles of KPE were agglomerated at the membrane center for the image of 50 ng KPE/mL composite (Figure 3A). The consistency and good distribution of the propolis components loaded on the composite appeared more clearly in the films containing 150 ng/mL concentrations (Figure 3C), followed by composite loading of 200 ng KPE/mL (Figure 3D), where the last composite reflects a chaos content of the KPE nanoparticles. The captures (Figures 3B,C) reflect far points of fractures, which link to the membrane permeability for the water vapor.

3.2 Assessment of film composite swelling ratio

The swelling ratio is the proportional increase in the composite mass attributable to hydration. After a crosslinking procedure, the polymer portion not incorporated into the crosslinked network is known as the sol fraction. The swelling behavior affects the composite film's mechanical characteristics and adsorption recovery. The swelling ratios are recorded for the two types of film composites (1:1 and 1:2) of CS to PVA concentrations every 30 min and up to 6 h (Figure 4A). The resistance-time interval is 210 and 300 min for the 1:1 CS-PVA and 1:2 CS-PVA, respectively. The composite of 1:2 CS-PVA has the highest swelling ratio at a 210-minute interval, degrading rapidly after this value. However, the swelling ratio reduction for the composite 1:1 CS-PVA after 300 min of the interval time is low. Up to these time intervals, no degradation was noticed in the film composite material of the two applied types. The composite swelling ratio could indicate several parameters if applied as a gel to derma healing sites. The composite swelling ratio could indicate several parameters if used as a gel to derma healing sites. This characteristic could help reduce skin wound water activity, leading to infection control.

3.3 Assessment of moisture retention capacity

Applied CS: PVA composite sheets of the two types (1:1 or 1:2) were evaluated for their moisture retention capacity values (Figure 4B). The moisture retention capacity determines the ability of the prepared film sheets to hold their moisture content

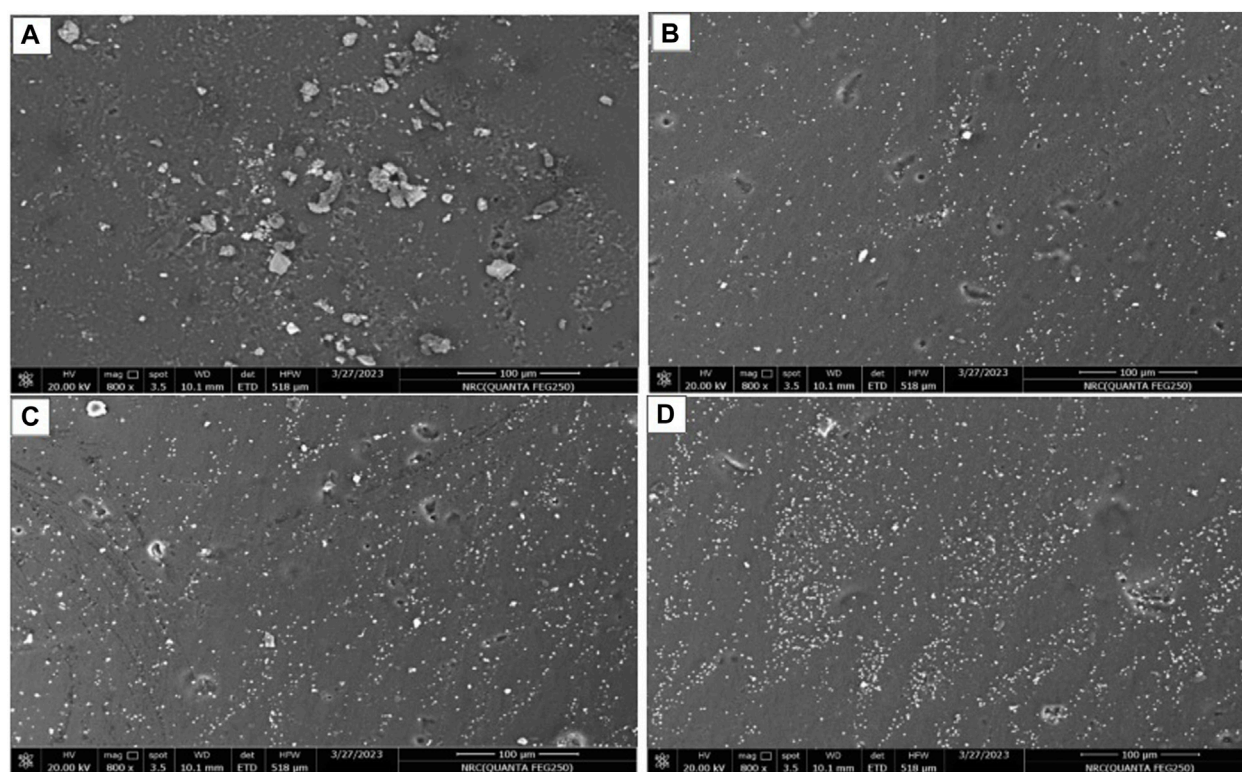


FIGURE 3

Scanning electron microscope of CS/PVA (1:1) loaded with KPE at concentrations of (A) 50 ng KPE/mL, (B) 100 KPE/mL, (C) 150 KPE/mL, and (D) 200 ng KPE/mL of nanoemulsion composite.

under outside influences such as heating. Up to a specific limit, this characteristic indicates how the film can stay elastic and resist damage during its utilization. In contrast, a high moisture capacity indicates more free water content, which affects microbial contamination. The results reflect that a film sheet containing an equal CS and PVA concentration has $65.21\% \pm 0.82\%$ as the MRC value. This was lower than the MRC value of the 1CS:2PVA film, which is $72.66\% \pm 1.81\%$ for the control film material. These values were increased through the insertion of propolis in the film composition.

The rate of the MRC increase was lower for the sheets of type 1CS:1PVA compared with the 1CS:2PVA sheets during the elevation of the inserted propolis concentration. Moreover, the changes recorded for the MRC values of the 1CS:1PVA sheet type for propolis concentrations were limited. In this regard, the previous results of the two sheet types (1:1 and 1:2 of the CS/PVA) could refer to the film containing equal concentrations as a more suitable sheet recommended for application in the following experimental steps.

3.4 Assessment of film color, thickness, and water activity

The film attributes are changed regarding the different concentrations of PVA applied to the film formation. The lightness (L^*), whiteness (a^*), and darkness (b^*) mostly

recorded changes in a comparison between CS: PVA (1:1 and 1: 2). Also, by enriching the film composite using propolis, its color attributes were influenced (Table 1). The value changes concerning the film color (ΔE) are shown to be incremental when raising KPE concentration content. The rate of ΔE elevation by propolis concentration doubled, which was noticeably more straightforward for the film composite with a higher PVA content. Significant changes were recorded for the film composite's color, with PVA and KPE concentrations. Generally, the formed composites prepared using CS/PVA and loading KPE concentrations have a color close to the skin. The thickness of CS-PVA composite films was assessed to measure the impact of PVA concentration changes (Table 1). The result is reflected by significant differences between the two composites (1: 1 and 1:2). No considerable changes are recorded for propolis insertion into the film composites except for CS-PVA at a concentration of (2:1) and just for KPE concentration of 200 ng/mL.

3.5 Assessment of thermal characteristics of loaded composites

The thermal characteristics of materials may be influenced by the combination of polymers and the addition of certain additives, a well-recognized fact. The effect of Korean Propolis extract (KPE), a bioactive component, on the thermal stability of

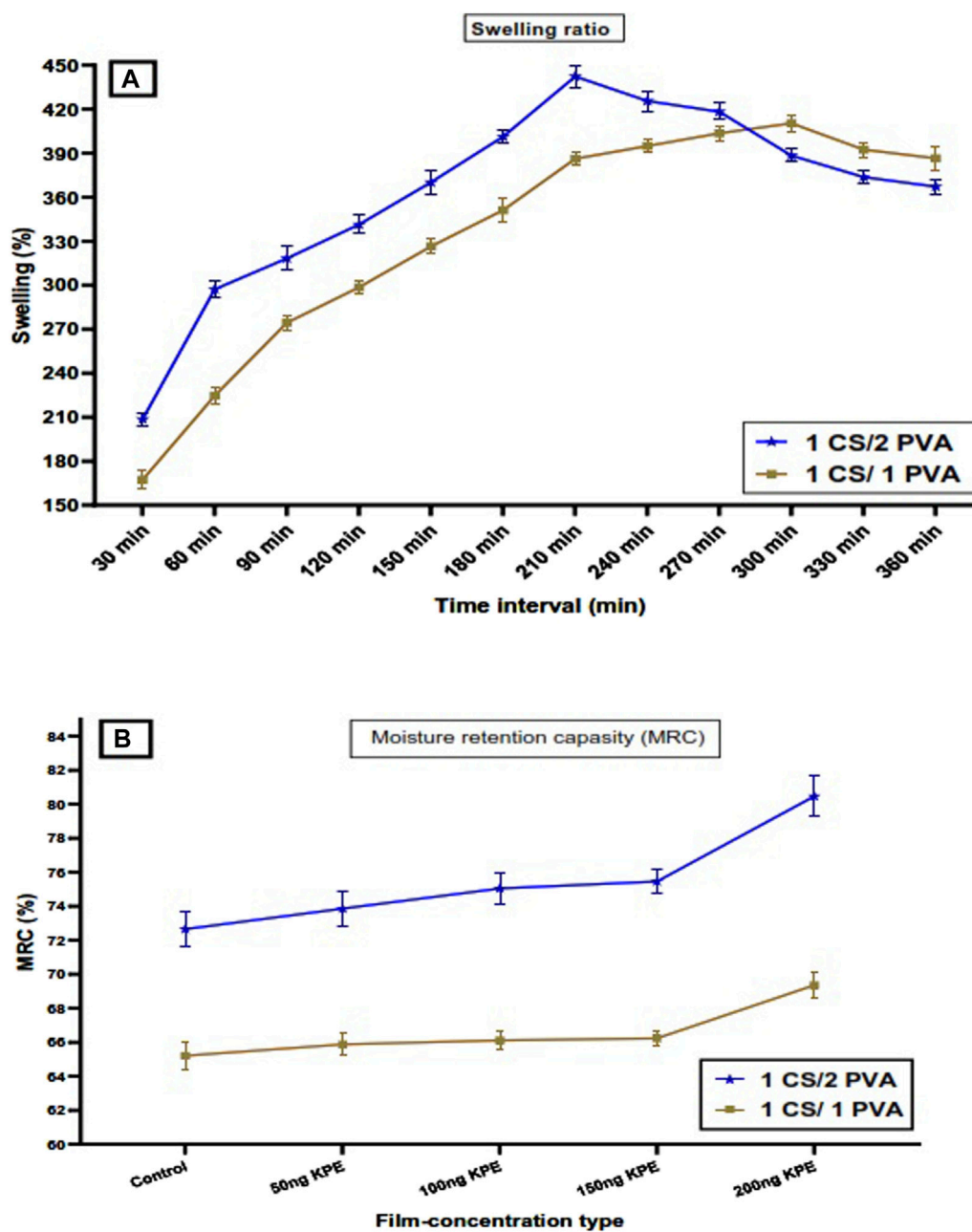


FIGURE 4 (A) Swelling properties and (B) moisture retention capacity of chitosan–polyvinyl alcohol composites at two different mixing ratios (CS: PVA; 1:1 and 1:2). KPE, Korean propolis extract; CS, chitosan; PVA, polyvinyl alcohol; MRC, moisture retention capacity.

PVA/CS composite at different concentrations is represented (Table 2). The reference indices used were the glass transition temperature (T_g), melting temperature (T_m), temperature of maximum breakdown rate (T_{max}), and the percentage of mass loss (at 300, 400, and 500°C). The results demonstrate that the composite stability significantly improved after loading with KPE compared to the original composite (PVA/CS). The Composite T_m values increased from 160°C to 168°C when loaded with KPE at a concentration of 50 ng/mL and up to 177°C when loaded with KPE at 200 ng/mL. The observed increases suggest that the structural semi-crystalline integrity of KPE's nanoparticles

could be impacted, perhaps due to the hydrogen bond generated between the molecules that formed the composite structure, where these bonds act as the backbone structure of the composite. The presence of these components may increase the formation of hydrogen bonds between the polymer chains, leading to a change in the organized structure of molecules in the film and indicating changes in crystallinity. Remarkably, the loaded bio-composite films of KPE exhibited greater T_{max} values than the reference composite, with T_{max} values of 327°C and 337°C. Besides, the residual content of the formed composite slightly increased at the same evaluation temperature. These

TABLE 1 Color attributes, thickness, and water activity changes of CS: PVA (1:1 or 1:2) as control composites or containing various KEP concentrations.

	L*	a*	b*	ΔE	Thickness (mm)	a_w
(1CS: 1 PVA) Film						
Control	73.05 ± 0.54 ^b	24.23 ± 0.28 ^a	34.25 ± 0.86 ^f	—	1.02 ± 0.05 ^a	0.37 ± 0.01 ^{ab}
50 ng KEP	55.61 ± 1.22 ^d	27.67 ± 1.16 ^b	31.37 ± 1.34 ^g	13.84	1.01 ± 0.04 ^a	0.34 ± 0.02 ^c
100 ng KEP	46.31 ± 1.37 ^g	28.94 ± 0.44 ^b	30.55 ± 0.88 ^h	24.29	1.04 ± 0.02 ^a	0.31 ± 0.02 ^d
150 ng KEP	44.21 ± 1.28 ^h	30.26 ± 0.55 ^d	28.94 ± 0.74 ^h	26.08	1.05 ± 0.04 ^a	0.32 ± 0.01 ^d
200 ng KEP	43.47 ± 1.18 ^k	30.79 ± 0.34 ^d	25.41 ± 0.91 ^k	25.67	1.07 ± 0.05 ^a	0.32 ± 0.02 ^{cd}
(1CS: 2PVA) Film						
Control	78.21 ± 0.37 ^a	14.71 ± 0.28 ^a	52.77 ± 1.02 ^a	—	0.85 ± 0.07 ^b	0.41 ± 0.02 ^b
50 ng KEP	62.44 ± 1.05 ^c	17.86 ± 0.41 ^f	49.37 ± 1.27 ^b	16.44	0.89 ± 0.04 ^b	0.37 ± 0.01 ^{ab}
100 ng KEP	56.77 ± 0.94 ^d	18.34 ± 0.34 ^f	46.55 ± 1.05 ^c	22.61	0.88 ± 0.06 ^b	0.38 ± 0.02 ^a
150 ng KEP	52.88 ± 0.54 ^e	20.41 ± 0.58 ^c	44.24 ± 1.14 ^d	27.12	0.91 ± 0.06 ^b	0.35 ± 0.02
200 ng KEP	50.18 ± 1.02 ^f	19.56 ± 0.45 ^c	41.37 ± 0.97 ^e	30.65	1.01 ± 0.05 ^a	0.36 ± 0.01 ^{bc}

Data are expressed as mean ± SD (SD: standard deviation; n = 3; $p \leq 0.05$). CS, chitosan; PVA, polyvinyl alcohol; KEP, Korean propolis extract. The values expressed with different superscript letters in the same column differ significantly. The values calculated as $\Delta E = \sqrt{(a^- - a)^2 + (b^- - b)^2 + (L^- - L)^2}$.

TABLE 2 TGA analysis of bio-composite polymeric materials of polyvinyl alcohol/chitosan (with/without propolis loading concentrations).

	T _g (°C)	T _m (°C)	T _{max} (°C)	Loss W ₁ (%)	Loss W ₂ (%)	Residue (%)
PVA/CS (1:1)	69	160	322	32	55	4.5
PVA/CS/KPE ₁	71	168	327	34	57	4.7
PVA/CS/KPE ₂	70	170	330	34	58	4.8
PVA/CS/KPE ₃	74	175	335	37	63	5.1
PVA/CS/KPE ₄	75	177	337	38	65	5.1

T, temperature; T_g, temperature of glass transition; T_m, temperature of melting; T_{max}, temperature of maximum decomposition rate; Loss W₁, %Weight loss at 300°C; Loss W₂, %Weight loss at 400°C; Residue (%): residue percentage of composite (at 500°C).

PVA/CS: a composite base of polyvinyl alcohol/chitosan at 1:1 (wt/wt); PVA/CS/KPE₁: a composite base loaded with 50 ng/mL of Korean propolis extract; KPE₂: a composite base loaded with 100 ng/mL of Korean propolis extract; KPE₃: a composite base loaded with 150 ng/mL of Korean propolis extract; KPE₄: a composite base loaded with 200 ng/mL of Korean propolis extract.

results could also be linked with formed bonds between the molecule contents after loading the KPE to composite and joined with the concentration increment of film.

The X-ray diffraction (XRD) patterns revealed clear and prominent peaks at an angle of $2\theta = 20^\circ$ – 50° . Significantly, peaks seen at 2θ values between 20° and 50° indicate the existence of chitosan at low KPE loading doses (Supplementary Figure S3). The thorough examination of XRD patterns offers valuable insights into the structural changes caused by including chitosan in the hybrid membranes, revealing the polymeric films' various crystalline and amorphous phases. The decrease in crystallinity seen in KPE-filled PVA/Cs composites may be attributed to the integration of KPE into the polymer matrix of the composite, together with the bioactive molecules. Incorporating KPE into PVA/CS composites affects the resulting composite structure's molecular arrangement and chain organization. The presence of extract ingredients from the KPE may initiate interactions with the composite chains, leading to the folding or rearranging of the chains and thus influencing the strength and frequency of these interactions.

3.6 Assessment of FTIR characteristics of 1CS:1PVA film

From this point forward, CS: PVA composite (1:1) was chosen as the recommended one to apply in further experiments. The Fourier transform infrared (FTIR) analysis showed the active group and functional sites of the 1CS:1 PVA film sheet when used as a control sheet or loaded with different amounts of propolis. The results reflect more active sites on the film sheet with the propolis loading concentration (Figure 5). The result reflected linking groups manifested with the film sheet's enrichment with propolis. Regarding the area of $1,000$ – $1,200$ cm^{-1} , groups of CH = CH were recorded in the form of cis ($1,054$ cm^{-1}) and trans ($1,137$ cm^{-1}) isomers, and their content was increased in association with the propolis concentration in the film sheet.

Also, the region between $1,500$ and 1700 cm^{-1} recorded contains several groups of C=O ($1,650$ cm^{-1}), O=C=O ($1,540$ cm^{-1}), and C=C ($1,670$ cm^{-1}), which could function by delivering the targeted materials. The area between 2800 and $3,000$ cm^{-1} indicates an increase in the film's active aldehyde and alcohol group content,

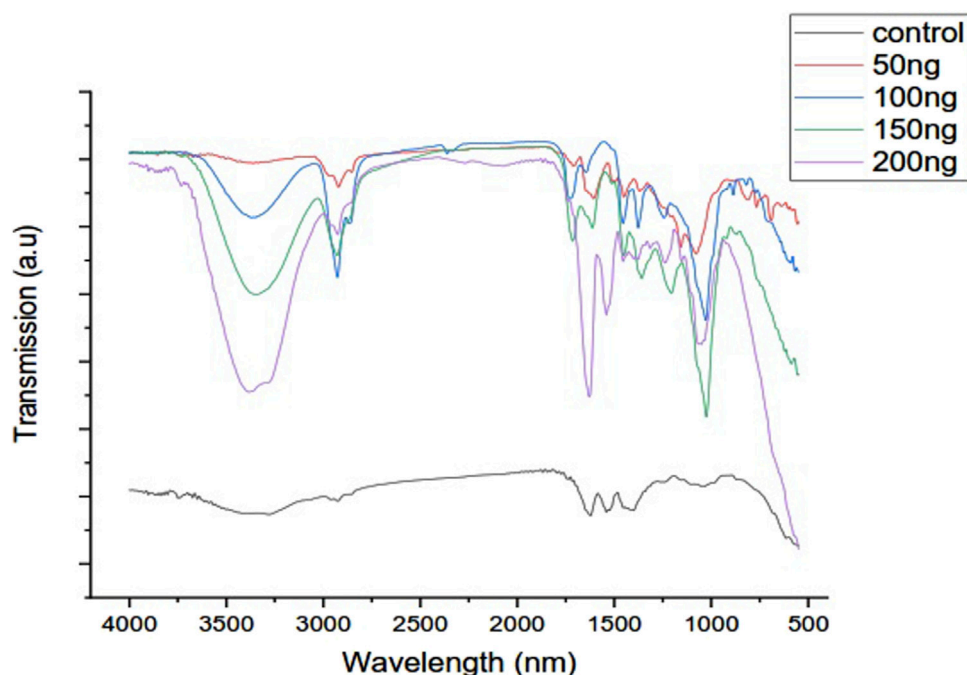


FIGURE 5
The FTIR evaluation of CS/PVA film sheet as control and with KPE (50, 100, 150, and 200 ng/mL). KPE, Korean propolis extract; CS, chitosan; PVA, polyvinyl alcohol.

which shows an increase in the content with an increasing concentration of propolis added to the film. The area between 3,200 and 3,500 cm^{-1} indicates the film membrane's hydroxyl group and carboxyl group contents, which have an essential function in the activity of the film membrane and its properties as a carrier medium for bioactive components that play a functional role when applied in medical and food applications.

The hydroxyl group, which manifests increased at 150 and 200 ng KPE/mL, plays a crucial role in nanoemulsions, especially in terms of stability and functionality; their importance is related to functionality such as stabilization, surface Activity, compatibility with Bioactive Compounds, improved bioavailability and antioxidant properties. The hydroxyl group plays an essential role in nanoemulsions' strength, functionality, and overall performance, delivering nanoparticles effective delivery systems for different purposes in cosmetics and pharmaceuticals.

The formation of chemical bonds in a nanoemulsion solution containing polyvinyl alcohol (PVA) and propolis extract is often attributed to hydrogen bonding. Hydrogen bonds are a specific kind of dipole-dipole interaction that arises when a hydrogen atom is covalently bound to an element with strong electronegativity due to electrostatic forces. These bonds are formed between the film material's PVA and chitosan, allowing KPE loading.

3.7 Antibacterial evaluation of loaded film materials

The results reflect considerable antibacterial properties of KPE-CS/PVA at the applied concentrations, particularly at 150 and

200 ng KPE/mL nanoemulsions (Figure 6). The assays of minimum inhibition concentration (MIC) and minimum bacterial concentration (MBC) are measured to represent the antimicrobial characteristics. Two bacterial strains of MRSA bacteria and *C. perfringens*, known to cause significant issues in wound contamination, are chosen to assess the nanoemulsions of KPE-CS/PVA. The composite with a propolis concentration of 150 ng/mL has antibacterial activity against the two strains, with no significant differences reported between the bacterial strains. Again, the values recorded regarding the MIC activities of the film loaded with 150 ng KPE/mL and 200 ng KPE/mL were shown to have close values. This result could recommend the application of 150 ng KPE/mL as the best treatment with high antimicrobial activity.

It is noticed that the higher the KPE-loading composite, the higher the antibacterial properties (MIC and MBC). In this regard, tested strains of bacteria that are known to form a biofilm and possess antibiotic resistance can positively inhibit using KPE-CS/PVA composite, particularly at KPE concentrations of 150 and 200 ng/mL. The result also reflects a more efficient 200 ng KPE composite against the strain of *C. perfringens*. The inhibition effect of the KPE-composite is close to that of the standard antibiotic azithromycin.

3.8 Anti-biofilm evaluation of CS/PVA-propolis

The application of the KPE-CS/PVA composite showed the capacity to inhibit the biofilm formation of test pathogen strains

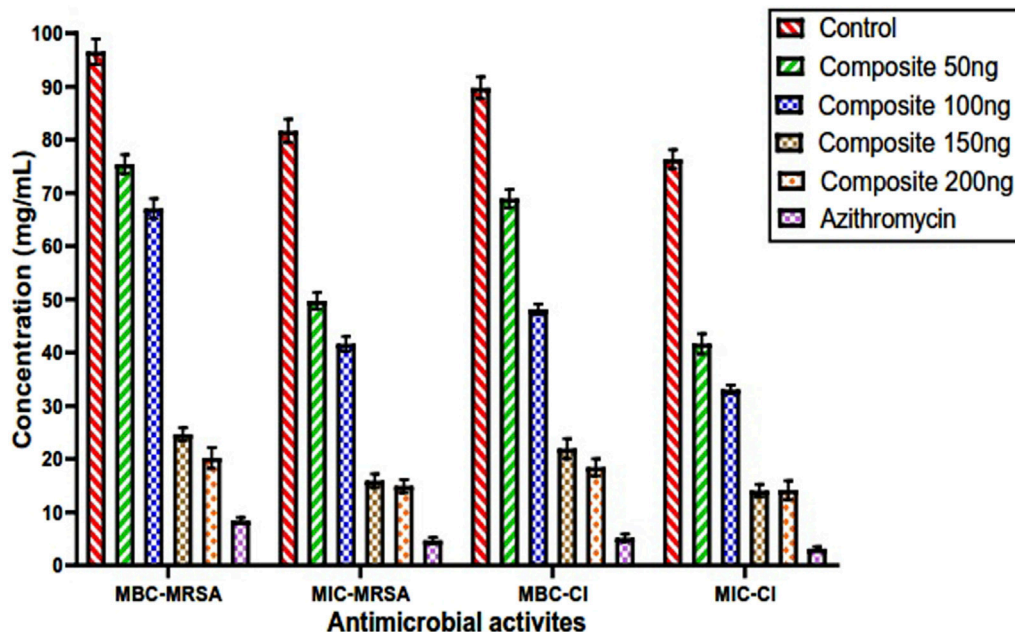


FIGURE 6

Minimum bacterial and minimum inhibition concentrations of the CS/PVA film (1:1) loaded by 50, 100, 150, and 200 ng KPE/mL compared to the control measured against two bacterial strains. KPE, Korean propolis extract; CS, chitosan; PVA, polyvinyl alcohol; MIC, minimal inhibitory concentration; MBC, minimal bactericidal concentration; MRSA, methicillin resistance *Staphylococcus aureus*.

(MRSA and *C. perfringens*), where the high efficiency is linked with more KPE concentrations (Figures 7A,B). It was noticed that the increment of the propolis concentration loaded onto CS/PVA composite material reflected more incredible bacterial anti-biofilm properties. The results indicated that CS/PVA-propolis concentrations of 150 and 200 ng KPE/mL closely impact the anti-biofilm characteristics. Also, these concentrations of propolis (150 and 200 ng/mL) were shown to be more effective in destroying the MRSA biofilm after a 4-h interval. Otherwise, the 150 ng KPE/mL concentration was found to kill the bacterial *Clostridium* biofilm after a 5-hour time interval. It was noticed that the antibiofilm properties of the composites against the two pathogens of the methicillin-resistant *Staphylococcus aureus* (Figure 7A) and *Clostridium perfringens* (Figure 7B) are close to each other, and the more efficiency recorded for 150 and 200 ng KPE-CS/PVA composites.

In the planktonic state, the bacteria are not attached to any surface and may be easily reached by the antimicrobial chemicals included in the KPE. This enables direct engagement and more effective disintegration of bacterial cells. The biofilms are intricate assemblages of bacteria that adhere to a surface and are immersed inside a self-generated matrix of extracellular polymeric substances (EPS). The matrix protects the bacteria from antimicrobial medications, reducing susceptibility to treatments compared to their planktonic counterparts. Bacteria inside a biofilm often exhibit a distinct metabolic state compared to planktonic bacteria. Therefore, they might exhibit reduced activity and be less susceptible to agents targeting actively proliferating cells. The EPS matrix can hinder the diffusion of antimicrobial agents, impeding their ability to reach the bacteria within the biofilm at effective concentrations. Bacteria associated with biofilms can

express distinct genes compared to free-floating bacteria, potentially including genes that resist antimicrobial substances. The combination of these features makes it more difficult for the antimicrobial components of KPE to penetrate and effectively combat bacteria in biofilm form, leading to reduced effectiveness compared to when the bacteria are in the planktonic condition. However, the composite of PVA/CS can act as a barrier that supports the antibiofilm impact of the applied KPE composite, forming a barrier and suppressing biofilm formation, which can illustrate the activity recorded in Figure 7 of the current results.

3.9 Animal experimental studies

Regarding the *in-vivo* application of KPE-CS/PVA composites, treating the infected would manifest an ameliorative impact, particularly at high KPE concentrations. Covering wounds with the composite gel affects the wound behavior of the MRSA-infecting load. Leg injuries with MRSA infection are shown rapidly in cases covered by KPE-CS/PVA gel of 150 ng KPE/mL composite. The results point out the efficiency of CS/PVA composites in accelerating wound curing, particularly when loaded with 150 ng/mL propolis. Compared to the standard antibiotic used in treatment, the results appeared to be based on a compound containing 150 mg of propolis, which was recorded to be close to the standard. In the G1, the rats were treated with CS/PVA film free of propolis nanoparticles, and the wound curing of the infected was slow compared to the rest of the treatments.

The wounds in this group showed the formation of simple purulent pockets and the appearance of suppurations, which were not recorded in the rest of the groups containing the propolis extract.

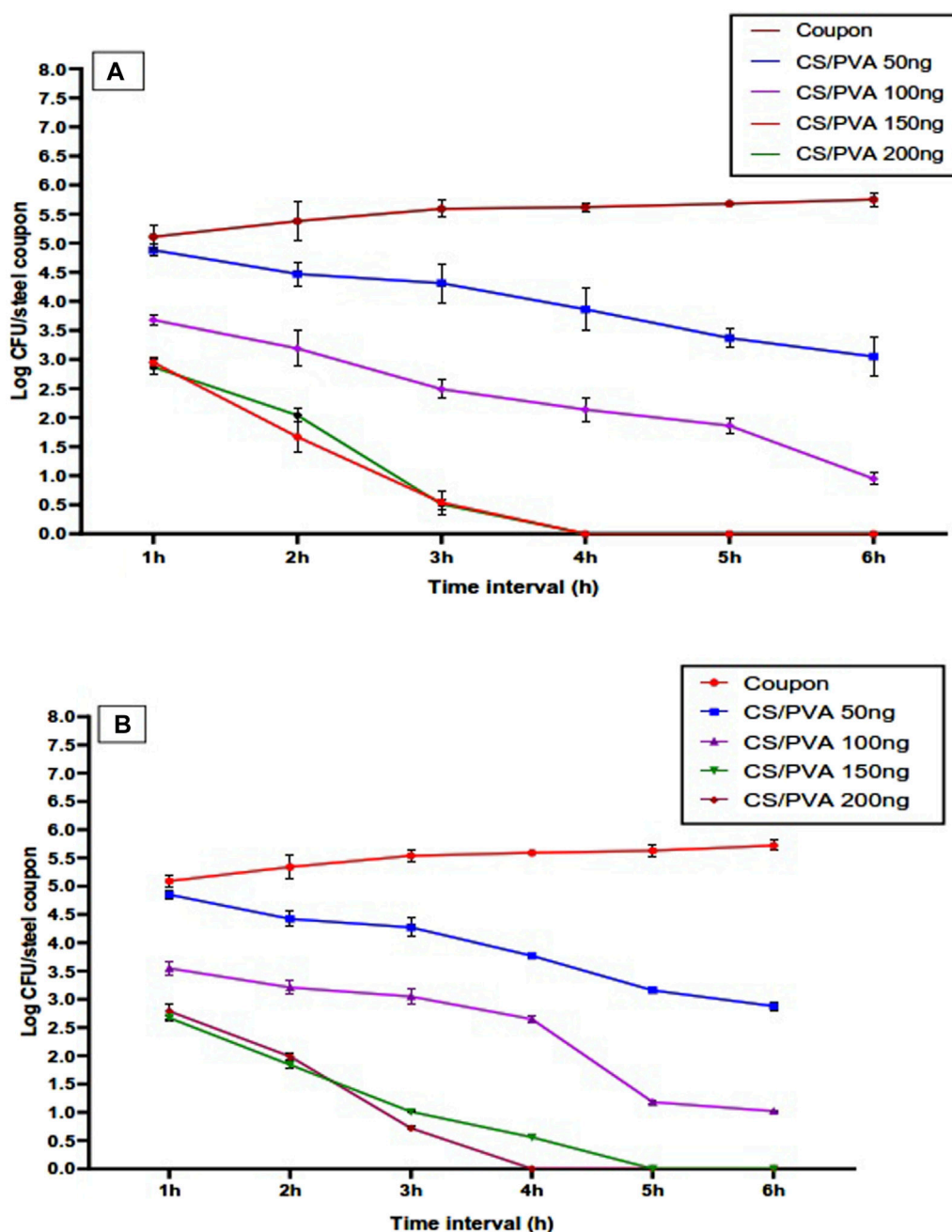


FIGURE 7

Anti-biofilm characteristics of the CS/PVA (1:1) loaded by 50, 100, 150, and 200 ng KPE/mL compared to the control measured against two bacterial strains. (A) Representation of bacterial-log count changes for methicillin-resistant *Staphylococcus aureus* regarding propolis concentration changes. (B) Representation of bacterial-log count changes for *Clostridium perfringens* regarding propolis concentration changes. KPE, Korean propolis extract; CS, chitosan; PVA, polyvinyl alcohol; CFU, colony forming unit.

A good response was recorded to treatments containing propolis, and these results were confirmed by evaluating the number of bacteria on the wounds daily and before covering them with the gel compound, by conducting bacterial swabs, and by assessing the total count (Supplementary Figure S1).

CS/PVA film loaded with 150 ng/mL treatment recorded better and more satisfactory results than the G2 rats treated with the standard antibiotic (Vancomycin). The G6 and G5 results were similar, with no significant improvement despite increased KEB

concentration with the G6 treatment. While the G3 (50 ng KPE/mL) and G4 (100 ng KPE/mL) treatments showed a specific improvement in the wounds infected with MRSA, this amelioration was less than that with the standard antibiotics (Vancomycin). The microbial load of wounds treated with propolis recorded a rapid deterioration in the number of MRSA bacteria on infected wounds, effectively contributing to the fast recovery of the affected skin cells. Reducing the bacterial load positively supported cell regeneration and increased the recovery rate of the affected areas.

In addition to the previous results, a special replicate was performed to compare the impact of 150 or 200 ng KPE/mL regarding the standard antibiotic effect. In this case, the infected injury has occurred in the dorsal area. A rapid improvement was observed in groups G5 and G6 compared to the rest groups during the treatment period. These results prompted the authors to repeat the experiment on several rats with a different injury area in the dorsal area instead of the front leg injury, as in the main experiment. Once again, the results showed that the treated rats with an injury area on the back showed a significant improvement in restoring the lost hair in the injury area and the recovery rate of the injured wounds. Also, the healing rate for the infection wound was the best for the G5 rats treated with CS/PVA loaded with 150 ng KPE/mL.

The swabbed of tested wound bacteria emphasizes the propolis's impact on decreasing MRSA infection. The results significantly reduced CS/PVA-propolis application on injury wounds. The total plate count of the infected injuries treated by CS/PVA-free was initiated with 2.71×10^5 CFU/mL on the second day of the treatment and recorded as 1.89×10^3 CFU/mL by the end of the treatment period. However, the results were infection-free after 5 days of CS/PVA-KPE treatment at 150 and 200 ng/mL. The MRSA infection needed more than 10 days to disappear from the injury with CS/PVA-KPE loaded at 50 and 100 ng/mL. These findings could emphasize the efficiency of KPE loading as a nanoemulsion with CS/PVA for curing the MRSA-infected injury and facilitating the healing properties.

4 Discussion

Chitosan is safe and has effective therapeutic properties, whereas PVA possesses biocompatibility, excellent processability, hydrophilicity, and attractive physical and chemical properties without affecting cells or organisms. PVA dissolves after long-term contact with polar fluids, making it challenging to employ separately in physiological and medical situations. Chitosan is the best polymer to blend with PVA to create a unique composite due to its antibacterial properties (Teodorescu et al., 2019; Kochkina and Lukin, 2020). Mixing PVA with CS improves control release and bioactivity (Liao et al., 2011; Mirzaeei et al., 2021). PVA was used to make a composite with CS since it does not impact chitosan's antibacterial capabilities (Cai et al., 2016; Annu and Ahmed, 2021). PVA/CS was utilized in the current study for the propolis loading, which helps protect the propolis active ingredients and limits their degradation.

Propolis extract is rich in bioactive components (phenolic and flavonoids) that significantly function for antimicrobial potency (Alarjani et al., 2023; Saleh et al., 2023). Propolis loading to PVA can improve anti-inflammation potential and enhance antimicrobial properties (Saleh et al., 2023). The present evaluation against pathogenic strains of bacteria shows this impact of inhibition. The PVA/CS loading with KPE was more effective at inhibiting *Staphylococcus aureus* and *Clostridium perfringens*, as demonstrated by the MIC, MBC, and antibiofilm on coupon tests (Figures 6, 7A,B). In this study, authors used two composite formulas of PVA/CS (1:1, 1:2) for loading propolis concentrations (50, 100, 150, and 200 ng/mL). The inter- and intramolecular KPE...Z (Z = halogen, oxygen, or nitrogen)

secondary interactions are expected to enhance the biological activity of propolis compounds (Dhau et al., 2021). However, compared to several KPE concentrations applied for the antimicrobial effect, the results reflected increased antibacterial potency by the KPE concentration elevation in the agar-diffusion well. This result may also illustrate the increment of active sites measured in the FT-IR results by raising KPE concentration (Figure 5). The nanoemulsion technique, particularly for antimicrobial and anti-pathogenic applications, can valorize the potency and efficiency of applied compounds (Singh et al., 2022). The mechanism of action for nanoemulsions may be linked to their efficiency against harmful bacteria through their valuable antioxidant impact or their impact against the reactive oxygen species.

In light of the graphical chart, the results demonstrate changes in composite material properties that make them more robust, more resistant to pressure, and able to stretch (Figure 2). Regarding the change in tensile stress, the CS/PVA film sheet has less dramatic changes due to the loading of KPE at different concentrations. Propolis nanoparticles explain this effect in the sheet that affected CS/PVA interaction. A previous investigation has mentioned the propolis' impact on film characterization with several changes (Olewnik-Kruszkowska et al., 2022). In the case of the 1CS/1PVA composite, the tensile stress dropped significantly from $33.74 + 0.44$ MPa to $27.05 + 0.66$ MPa for the composite. The tensile stress values decreased from $29.77 + 0.39$ to $21.55 + 0.81$ MPa in the 1CS/2PVA composite.

It was also clear that the tensile stress values changed more quickly as KPE concentration increased in the 1CS/2PVA composite material (Figure 2A). The observed reduction can be attributed to the dispersion of propolis molecules, reducing the film matrix's cohesive forces. According to (Šuran et al., 2021), an increased distribution of KPE content leads to decreased cohesive forces and composite strength. Previous research has also shown that the tensile stress value decreases with more component loading on the composite materials (Ahmad et al., 2015; Suriyatem et al., 2019). The changes in the tensile stress values may be linked to other changes in the mechanical properties of the formed film. These properties were the elasticity and elongation at break (Figures 2B,C). A similar result was reported in several studies, where these composites also contained chitosan as one of the ingredients (Pinzon et al., 2018). The fact that they are associated with more water and lower tensile strength helps to explain the slight changes in elastic modulus and elongation at break values. The water content increases in the composite content were clarified due to the presence of PVA and its ratio in the film content (Khonakdar et al., 2003; Talja et al., 2007).

Otherwise, the composite sheet thickness recorded was less for 1CS/2PVA than for 1CS/1PVA, even when the composite was loaded with the different KPE concentrations. The attributes of the composites loaded with different KPE concentrations provide degrees of color very close to the skin's color (Table 1), which gives a chance for their probable skin application. The water activities of 1CS/1 PVA composites were lower than those of 1CS/2 PVA sheets, while the last one's capacity to absorb water was higher. The limited availability of the water molecules is due to their insertion into the 1:1 CS/PVA composite structure, which explains this point. The formed sheets' swelling ratio and water

retention capacity reflect their resistance to rapid degradation (Figures 4A,B). These characteristics could be significant for bioactive material delivery systems (Vishal Gupta and Shivakumar, 2010; Lv et al., 2019).

Significant chitosan and polyvinyl alcohol content of active groups (NH₂, OH, C-H) play a functional role in the form of the bonds formed with the Korean propolis that was loaded (Figure 5). These groups provide several hydrogen bonds with loaded KPE extract, increasing its effectiveness, protection against degradation, and effectively controlling its delivery. It was clear that there was a change in the active group contents of the compound and the occurrence of bonds with the change in the concentration of the loaded extract. The higher KPE concentration reflects the higher active group content, which aids in the conductivity properties of the composite (Hou et al., 2013; Chen et al., 2018). The composites of loaded KPE showed significant activity against pathogenic microorganisms of MRSA and *C. perfringens* strains, which are known to cause severe wound infections. Depending on the effect of dose importance and economy, these results support the application of 150 ng KPE/mL for medical and pharmaceutical purposes, as results recorded close values for concentrations of 150 and 200 ng KPE/mL composite.

Because the biofilm matrix protects the bacteria, the biofilm is more antibiotic-resistant. The current research found considerable bacterial biofilm suppression, possibly due to KPE's protective effect and the PVA/CS's barrier effect. This research assessed the KPE composite's anti-biofilm properties using laminar flow. Laminar flow suits biological systems best. Turbulent or laminar flow may impact biofilm-forming microbe gene expression (Tsagkari et al., 2022). In laminar flow (stable state), bacteria may better control their genes by concentrating on growth and maintenance rather than stress (Kalia et al., 2023; Sadeghzadeh et al., 2024). These circumstances alleviate stress and enable regulated EPS generation, creating organized biofilms with layers and channels (Pan et al., 2022). However, turbulent flow activates genes and upregulates biofilm-forming adhesion factors and EPS. Bacterial gene expression may differ under both flow conditions.

The CS dressings were applied to heal the skin because of their ease of application, antibacterial and hemostatic properties, and capacity to encourage skin regeneration. The CS can clean wound bacterial infection during inflammation and promote granulation tissue formation to speed skin proliferation (Feng et al., 2021). The CS is crucial to wound healing's hemostasis, inflammation, and proliferation (Xia et al., 2022). In our study, this characteristic plays a significant role in wound healing, besides its functionality and KPE deliverability. The anti-inflammatory substances in propolis extract help reduce pain, heat, and swelling at the wound site, making it easier for the wound to heal.

Wound dressings benefit from exudate absorbents with high swelling capacity and porosity, water vapor transfer, antibacterial and anti-inflammatory properties, and low germ permeability. These properties were attained in KPE-CS/PVA nanocomposites (Figures 2, 3; Table 1). Most commercial dressings lack elasticity, flexibility, medication loading, tensile strength, spreadability, and the ability to moisten wounds to hasten healing. These effects were crucial to achieving the stated goals of increasing wound healing response and reducing microbial burden in infected sites. KPE-containing composites reduce hazardous bacteria biofilm formation and were proven to be effective. Comparing coupon test inhibition time before and after bacteria addition showed this result. The compositions with

150 and 200 ng KPE/mL composite inhibited significantly (Figures 6, 7A, B). Vancomycin demonstrated similar effects to propolis (150 and 200 ngKPE/mL) composites in treating dorsal injuries and hair loss in rats (Supplementary Figure S2). These data support propolis's *staphylococcus aureus*-reducing efficacy (Abdelsattar et al., 2022). After 8 days of Vancomycin and KPE composite treatments, the afflicted regions saw significant hair growth. These findings prove the potential of these molecules to prevent bacterial infection and aid skin restoration. Swabbing afflicted regions every 4 days and monitoring bacteria growth on Petri plates verified the outcomes.

5 Conclusion

This research utilized 1:1 and 1:2 chitosan (CS)/polyvinyl alcohol (PVA) loading materials. As co-surfactants, glycerol and sorbitol improved the composite's characteristics. The 1:1 CS/PVA mixture was marked significantly after loading with Korean propolis extract. Composite mechanical characteristics differ between 1 CS/1 and 1 CS/2 PVA formulations. Increasing KPE concentration did not influence sheet thickness, even if water activity was reduced. Adding KPE gives composites more active FTIR groups, helping provide bioactive components. MRSA and *Clostridium* bacteria, wound pathogens, were most effectively inhibited by composites containing 150 or 200 ng KPE/mL. Antibacterial action may be enhanced by CS bioactivity. The composites also inhibited biofilm growth at these concentrations. In animal tests, KPE-loaded composites (150 or 200 ng KPE/mL) eradicate MRSA infection. The best results were at 150 ng KPE/mL. Combining treatment against leg and dorsal infected locations boosted efficiency ratings. Microbiological swabs from wounds treated with KPE-loading composites improved significantly in a total plate count test for MRSA infection. These data showed that 1 CS/1 PVA with 150 ng KPE/mL was the best wound-MRSA infection therapy and wound-healing assistance. The composite treated skin infections without affecting wound aesthetics.

Data availability statement

The raw data supporting the conclusions of this article will be made available by the authors, without undue reservation.

Ethics statement

The animal study was approved by the Institutional Ethics Committee of King Saud University (protocol code KSU-SE-22-124) on 29 January 2023. The study was conducted in accordance with local legislation and institutional requirements. The study was conducted in accordance with the local legislation and institutional requirements.

Author contributions

KA: Conceptualization, Data curation, Funding acquisition, Project administration, Resources, Software, Supervision, Visualization, Writing—original draft. HY: Conceptualization, Data curation, Funding acquisition, Project administration, Resources, Software,

Supervision, Validation, Visualization, Writing—original draft. AB: Data curation, Formal Analysis, Investigation, Methodology, Software, Writing—original draft, Writing—review and editing. HA: Data curation, Formal Analysis, Investigation, Methodology, Validation, Writing—original draft. AA-M: Data curation, Resources, Software, Validation, Visualization, Writing—original draft. SaA: Formal Analysis, Software, Validation, Visualization, Writing—original draft. ShA: Formal Analysis, Investigation, Software, Validation, Visualization, Writing—original draft. AR: Data curation, Formal Analysis, Software, Visualization, Writing—original draft. MA-M: Data curation, Validation, Visualization, Software, Writing—original draft.

Funding

The author(s) declare that financial support was received for the research, authorship, and/or publication of this article. The authors extend their appreciation to the Deputyship for Research & Innovation, Ministry of Education in Saudi Arabia for funding this research work through the project no. (IFKSUDR_H260).

Conflict of interest

The authors declare that the research was conducted in the absence of any commercial or financial relationships that could be construed as a potential conflict of interest.

Publisher's note

All claims expressed in this article are solely those of the authors and do not necessarily represent those of their affiliated organizations, or those of the publisher, the editors and the

reviewers. Any product that may be evaluated in this article, or claim that may be made by its manufacturer, is not guaranteed or endorsed by the publisher.

Supplementary material

The Supplementary Material for this article can be found online at: <https://www.frontiersin.org/articles/10.3389/fnano.2024.1387933/full#supplementary-material>

SUPPLEMENTARY FIGURE S1

An animal experimental study of CS/PVA loaded with KPE at different concentrations for wounds infected with the MRSA bacteria and treated for 18 days. The figure shown selected images for groups (G3): rats with leg injuries had MRSA infection treated with propolis (50 ng/mL); (G4): rats with leg injuries had MRSA infection treated with propolis (100 ng/mL); (G5): rats with leg injuries had MRSA infection treated with propolis (150 ng/mL); (G6): rats with leg injuries had MRSA infection treated with propolis (200 ng/mL).

SUPPLEMENTARY FIGURE S2

Animal experimental study of CS/PVA loaded with KPE at the concentration of 150 and 200 ng/mL for wounds infected with the MRSA bacteria and treated for 18 days. (G2): Rats with dorsal injuries had MRSA infection treated by Vancomycin (150 ng); (G5): rats with dorsal injuries had MRSA infection treated with propolis (150 ng/mL); (G6): rats with dorsal injuries had MRSA infection treated with propolis (200 ng/mL). The blue arrow referred to the wound infected place after treatment.

SUPPLEMENTARY FIGURE S3

XRD pattern of PVA/CS composite at different KPE concentrations. PVA, polyvinyl alcohol; CS, chitosan; KPE, Korean propolis extract.

SUPPLEMENTARY FIGURE S4

Selected photo for inhibition zones diameters of the PVA/CS/KPE composite nanoemulsion against (A) *Staphylococcus aureus* (B) *C. perfringens* strains of bacteria. Orange arrow : PVA/CS at 200 ng/mL KPE; blue arrow : PVA/CS at 150 ng/mL KPE.

SUPPLEMENTARY FIGURE S5

Selected photo for the swelling behavior of KPE composite loaded into composite film formed using two formulas of PVA/CS (1:1 and 2:1).

References

- Abdelsattar, A. S., Makky, S., Nofal, R., Hebshy, M., Agwa, M. M., Aly, R. G., et al. (2022). Enhancement of wound healing via topical application of natural products: *in vitro* and *in vivo* evaluations. *Arabian J. Chem.* 15, 103869–103920. doi:10.1016/j.arabjc.2022.103869
- Ahmad, M., Hani, N. M., Nirmal, N. P., Fazial, F. F., Mohtar, N. F., and Romli, S. R. (2015). Optical and thermo-mechanical properties of composite films based on fish gelatin/rice flour fabricated by casting technique. *Prog. Org. Coatings* 84, 115–127. doi:10.1016/j.porgcoat.2015.02.016
- Alarjani, K. M., Yehia, H. M., Badr, A. N., Ali, H. S., Al-Masoud, A. H., Alhaqbani, S. M., et al. (2023). Anti-MRSA and biological activities of propolis concentrations loaded to chitosan nanoemulsion for pharmaceutical applications. *Pharmaceutics* 15, 2386. doi:10.3390/pharmaceutics15102386
- Almeida, E. T., Da Silva, M. C. D., Oliveira, J. M. D. S., Kamiya, R. U., Arruda, R., Elleson, D. S., et al. (2017). Chemical and microbiological characterization of tinctures and microcapsules loaded with Brazilian red propolis extract. *J. Pharm. Analysis* 7, 280–287. doi:10.1016/j.jpaha.2017.03.004
- Amalaradjou, M. A., and Venkitanarayanan, K. (2014). Antibiofilm effect of octenidine hydrochloride on *Staphylococcus aureus*, MRSA and VRSA. *Pathogens* 3, 404–416. doi:10.3390/pathogens3020404
- Amalaradjou, M. A. R., Narayanan, A., Baskaran, S. A., and Venkitanarayanan, K. (2010). Antibiofilm effect of trans-cinnamaldehyde on uropathogenic *Escherichia coli*. *J. Urology* 184, 358–363. doi:10.1016/j.juro.2010.03.006
- Annu, A. A., and Ahmed, S. (2021). Eco-friendly natural extract loaded antioxidative chitosan/polyvinyl alcohol based active films for food packaging. *Heliyon* 7, 1–24. doi:10.1016/j.heliyon.2021.e06550
- Barzegar, S., Zare, M. R., Shojaei, F., Zarehsharabadi, Z., Koohi-Hosseiniabadi, O., Saharkhiz, M. J., et al. (2021). Core-shell chitosan/PVA-based nanofibrous scaffolds loaded with *Satureja mutica* or *Oliveria decumbens* essential oils as enhanced antimicrobial wound dressing. *Int. J. Pharm.* 597, 120288–121208. doi:10.1016/j.ijpharm.2021.120288
- Bhatia, A., Saikia, P. P., Dkhar, B., and Pyngrope, H. (2022). Anesthesia protocol for ear surgery in Wistar rats (animal research). *Animal Models Exp. Med.* 5, 183–188. doi:10.1002/ame2.12198
- Boateng, J., and Catanzano, O. (2015). Advanced therapeutic dressings for effective wound healing—a review. *J. Pharm. Sci.* 104, 3653–3680. doi:10.1002/jps.24610
- Boisard, S., Le Ray, A.-M., Landreau, A., Kempf, M., Cassisa, V., Flurin, C., et al. (2015). Antifungal and antibacterial metabolites from a French poplar type propolis. *Evidence-Based Complementary Altern. Med.* 2015, 1–10. doi:10.1155/2015/319240
- Cai, J., Chen, J., Zhang, Q., Lei, M., He, J., Xiao, A., et al. (2016). Well-aligned cellulose nanofiber-reinforced polyvinyl alcohol composite film: mechanical and optical properties. *Carbohydr. Polym.* 140, 238–245. doi:10.1016/j.carbpol.2015.12.039
- Cao, N., Fu, Y., and He, J. (2007). Mechanical properties of gelatin films crosslinked, respectively, by ferulic acid and tannin acid. *Food Hydrocoll.* 21, 575–584. doi:10.1016/j.foodhyd.2006.07.001
- Cárdenas, G., Anaya, P., Del Rio, R., Schrebler, R., Von Plessing, C., and Schneider, M. (2010). Scanning electron microscopy and atomic force microscopy of chitosan composite films. *J. Chil. Chem. Soc.* 55, 352–354. doi:10.4067/S0717-97072010000300017

- Chen, W., Zhou, S., Ge, L., Wu, W., and Jiang, X. (2018). Translatable high drug loading drug delivery systems based on biocompatible polymer nanocarriers. *Biomacromolecules* 19, 1732–1745. doi:10.1021/acs.biomac.8b00218
- Dhau, J. S., Singh, A., Brandão, P., and Felix, V. (2021). Synthesis, characterization, X-ray crystal structure and antibacterial activity of bis[3-(4-chloro-N,N-diethylpyridine-2-carboxamide)] diselenide. *Inorg. Chem. Commun.* 133, 108942. doi:10.1016/j.inoche.2021.108942
- Dzhalo, M., Mierziak, J., Korzun, U., Preisner, M., Szopa, J., and Kulma, A. (2016). The potential of plant phenolics in prevention and therapy of skin disorders. *Int. J. Mol. Sci.* 17, 160. doi:10.3390/ijms17020160
- El-Seedi, H. R., Eid, N., Abd El-Wahed, A. A., Rateb, M. E., Afifi, H. S., Algethami, A. F., et al. (2022). Honey bee products: preclinical and clinical studies of their anti-inflammatory and immunomodulatory properties. *Front. Nutr.* 8, 1–26. doi:10.3389/fnut.2021.761267
- Feng, P., Luo, Y., Ke, C., Qiu, H., Wang, W., Zhu, Y., et al. (2021). Chitosan-based functional materials for skin wound repair: mechanisms and applications. *Front. Bioeng. Biotechnol.* 9, 650598–650636. doi:10.3389/fbioe.2021.650598
- Grada, A., Mervis, J., and Falanga, V. (2018). Research techniques made simple: animal models of wound healing. *J. Investigative Dermatol.* 138, 2095–2105.e1. doi:10.1016/j.jid.2018.08.005
- Hou, Z., Li, Y., Huang, Y., Zhou, C., Lin, J., Wang, Y., et al. (2013). Phytosomes loaded with mitomycin C-soybean phosphatidylcholine complex developed for drug delivery. *Mol. Pharm.* 10, 90–101. doi:10.1021/mp300489p
- Hu, D., Qiang, T., and Wang, L. (2017). Quaternized chitosan/polyvinyl alcohol/sodium carboxymethylcellulose blend film for potential wound dressing application. *Wound Med.* 16, 15–21. doi:10.1016/j.wndm.2016.12.003
- Kalantari, K., Mostafavi, E., Saleh, B., Soltantabar, P., and Webster, T. J. (2020). Chitosan/PVA hydrogels incorporated with green synthesized cerium oxide nanoparticles for wound healing applications. *Eur. Polym. J.* 134, 109853–110113. doi:10.1016/j.eurpolymj.2020.109853
- Kalia, V. C., Patel, S. K. S., and Lee, J.-K. (2023). Bacterial biofilm inhibitors: an overview. *Ecotoxicol. Environ. Saf.* 264, 115389. doi:10.1016/j.ecoenv.2023.115389
- Kalia, A., Kaur, M., Shami, A., Jawandha, S. K., Alghuthaymi, M. A., Thakur, A., et al. (2021). Nettle-leaf extract derived ZnO/CuO nanoparticle-biopolymer-based antioxidant and antimicrobial nanocomposite packaging films and their impact on extending the post-harvest shelf life of guava fruit. *Biomolecules* 11, 224. doi:10.3390/biom11020224
- Khandia, R., Puranik, N., Bhargava, D., Lodhi, N., Gautam, B., and Dhama, K. (2021). Wound infection with multi-drug resistant clostridium perfringens: a case study. *Archives Razi Inst.* 76, 1565–1573. doi:10.22092/ari.2021.355985.1757
- Khonakdar, H. A., Morshedani, J., Wagenknecht, U., and Jafari, S. H. (2003). An investigation of chemical crosslinking effect on properties of high-density polyethylene. *Polymer* 44, 4301–4309. doi:10.1016/S0032-3861(03)00363-X
- Kim, H., Park, S.-Y., and Lee, G. (2019). Potential therapeutic applications of bee venom on skin disease and its mechanisms: a literature review. *Toxins* 11, 374. doi:10.3390/toxins11070374
- Kochkina, N. E., and Lukin, N. D. (2020). Structure and properties of biodegradable maize starch/chitosan composite films as affected by PVA additions. *Int. J. Biol. Macromol.* 157, 377–384. doi:10.1016/j.ijbiomac.2020.04.154
- Kurek-Górecka, A., Rzepecka-Stojko, A., Górecki, M., Stojko, J., Sosada, M., and Świerczek-Zięba, G. (2014). Structure and antioxidant activity of polyphenols derived from propolis. *Molecules* 19, 78–101. doi:10.3390/molecules19010078
- Liao, H., Qi, R., Shen, M., Cao, X., Guo, R., Zhang, Y., et al. (2011). Improved cellular response on multiwalled carbon nanotube-incorporated electrospun polyvinyl alcohol/chitosan nanofibrous scaffolds. *Colloids Surfaces B Biointer.* 84, 528–535. doi:10.1016/j.colsurfb.2011.02.010
- Lv, Q., Wu, M., and Shen, Y. (2019). Enhanced swelling ratio and water retention capacity for novel super-absorbent hydrogel. *Colloids Surfaces A Physicochem. Eng. Aspects* 583, 123972–124142. doi:10.1016/j.colsurfa.2019.123972
- Maham, A., Tang, Z., Wu, H., Wang, J., and Lin, Y. (2009). Protein-based nanomedicine platforms for drug delivery. *Small* 5, 1706–1721. doi:10.1002/smll.200801602
- Maureen, U. O., Mitsan, O., Augustine, O. A., and Osazee, E. I. (2019). Methicillin-resistant *Staphylococcus aureus* (MRSA) and anti-MRSA activities of extracts of some medicinal plants: a brief review. *AIMS Microbiol.* 5, 117–137. doi:10.3934/microbiol.2019.2.117
- Mirzaeei, S., Taghe, S., Asare-Addo, K., and Nokhodchi, A. (2021). Polyvinyl alcohol/chitosan single-layered and polyvinyl alcohol/chitosan/eudragit RL100 multi-layered electrospun nanofibers as an ocular matrix for the controlled release of ofloxacin: an *in vitro* and *in vivo* evaluation. *AAPS Pharm. Sci. Tech.* 22, 170–188. doi:10.1208/s12249-021-02051-5
- Narayanan, A., Nair, M. S., Karumathil, D. P., Baskaran, S. A., Venkitanarayanan, K., and Amalaradjou, M. A. R. (2016). Inactivation of acinetobacter baumannii biofilms on polystyrene, stainless steel, and urinary catheters by octenidine dihydrochloride. *Front. Microbiol.* 7, 847–936. doi:10.3389/fmicb.2016.00847
- Naskar, A., and Kim, K.-S. (2020). Recent advances in nanomaterial-based wound-healing therapeutics. *Pharmaceutics* 12, 499. doi:10.3390/pharmaceutics12060499
- Olewnik-Kruszkowska, E., Gierszewska, M., Wrona, M., Nerin, C., and Grabska-Zielińska, S. (2022). Polylactide-based films with the addition of poly (ethylene glycol) and extract of propolis—physico-chemical and storage properties. *Foods* 11, 101488. doi:10.3390/foods11101488
- Oryan, A., Alemzadeh, E., and Moshiri, A. (2018). Potential role of propolis in wound healing: biological properties and therapeutic activities. *Biomed. Pharmacother.* 98, 469–483. doi:10.1016/j.biopha.2017.12.069
- Otoni, C. G., Moura, M. R. D., Aouada, F. A., Camilloto, G. P., Cruz, R. S., Lorevice, M. V., et al. (2014). Antimicrobial and physical-mechanical properties of pectin/papaya puree/cinnamaldehyde nanoemulsion edible composite films. *Food Hydrocoll.* 41, 188–194. doi:10.1016/j.foodhyd.2014.04.013
- Pan, M., Li, H., Han, X., Ma, W., Li, X., Guo, Q., et al. (2022). Effects of hydrodynamic conditions on the composition, spatiotemporal distribution of different extracellular polymeric substances and the architecture of biofilms. *Chemosphere* 307, 135965. doi:10.1016/j.chemosphere.2022.135965
- Pascoal, A., Feás, X., Dias, T., Dias, L. G., and Estevinho, L. M. (2014). “Chapter 13 - the role of honey and propolis in the treatment of infected wounds,” in *Microbiology for surgical infections*. Editors K. Kon and M. Rai (Amsterdam, Netherlands: Academic Press). doi:10.1016/B978-0-12-411629-0.00013-1
- Percival, S. L., Hill, K. E., Williams, D. W., Hooper, S. J., Thomas, D. W., and Costerton, J. W. (2012). A review of the scientific evidence for biofilms in wounds. *Wound Repair Regen.* 20, 647–657. doi:10.1111/j.1524-475X.2012.00836.x
- Pinzon, M. I., Garcia, O. R., and Villa, C. C. (2018). The influence of Aloe vera gel incorporation on the physicochemical and mechanical properties of banana starch-chitosan edible films. *J. Sci. Food Agric.* 98, 4042–4049. doi:10.1002/jsfa.8915
- Pisoschi, A. M., Pop, A., Cimpeanu, C., Turcuș, V., Predoi, G., and Iordache, F. (2018). Nanoencapsulation techniques for compounds and products with antioxidant and antimicrobial activity - a critical view. *Eur. J. Med. Chem.* 157, 1326–1345. doi:10.1016/j.ejmech.2018.08.076
- Pobiega, K., Gniewosz, M., and Krasniewska, K. (2017). Antimicrobial and antiviral properties of different types of propolis. *Zesz. Probl. Postępów Nauk. Rol.* 9, 69–79. doi:10.22630/ZPPNR.2017.589.22
- Ribeiro, A. M., Estevinho, B. N., and Rocha, F. (2021). Preparation and incorporation of functional ingredients in edible films and coatings. *Food Bioprocess Technol.* 14, 209–231. doi:10.1007/s11947-020-02528-4
- Risha Achaiah, I., Gayathri, B. H., Banu, N., Kaliprasad, C. S., Beena Ullala Mata, B. N., Ajeya, K. P., et al. (2023). Efficient removal of metal ions from aqueous solutions using MoS₂ functionalized chitosan Schiff base incorporated with Fe₃O₄ nanoparticle. *Int. J. Biol. Macromol.* 248, 125976. doi:10.1016/j.ijbiomac.2023.125976
- Sadeghzadeh, R., Esfandiari, Z., Khaneghah, A. M., and Rostami, M. (2024). A review of challenges and solutions of biofilm formation of *Escherichia coli*: conventional and novel methods of prevention and control. *Food Bioprocess Technol.* doi:10.1007/s11947-023-03288-7
- Salatino, A. (2022). Perspectives for uses of propolis in therapy against infectious diseases. *Molecules* 27, 4594. doi:10.3390/molecules27144594
- Saleh, S., Salama, A., Ali, A. M., Saleh, A. K., Elhady, B. A., and Tolba, E. (2023). Egyptian propolis extract for functionalization of cellulose nanofiber/poly(vinyl alcohol) porous hydrogel along with characterization and biological applications. *Sci. Rep.* 13, 7739. doi:10.1038/s41598-023-34901-6
- Singh, B. N., Panda, N. N., Mund, R., and Pramanik, K. (2016). Carboxymethyl cellulose enables silk fibroin nanofibrous scaffold with enhanced biomimetic potential for bone tissue engineering application. *Carbohydr. Polym.* 151, 335–347. doi:10.1016/j.carbpol.2016.05.088
- Singh, A., Singh, P., Kumar, R., and Kaushik, A. (2022). Exploring nanoselenium to tackle mutated SARS-CoV-2 for efficient COVID-19 management. *Front. Nanotechnol.* 4, 1004729. doi:10.3389/fnano.2022.1004729
- Sun, L., Sun, J., Chen, L., Niu, P., Yang, X., and Guo, Y. (2017). Preparation and characterization of chitosan film incorporated with thinned young apple polyphenols as an active packaging material. *Carbohydr. Polym.* 163, 81–91. doi:10.1016/j.carbpol.2017.01.016
- Šuran, J., Cepanec, I., Mašek, T., Radić, B., Radić, S., Tlak Gajger, I., et al. (2021). Propolis extract and its bioactive compounds—from traditional to modern extraction technologies. *Molecules* 26, 2930. doi:10.3390/molecules26102930
- Suriyatem, R., Auras, R. A., and Rachtanapun, P. (2019). Utilization of carboxymethyl cellulose from durian rind agricultural waste to improve physical properties and stability of rice starch-based film. *J. Polym. Environ.* 27, 286–298. doi:10.1007/s10924-018-1343-z
- Talja, R. A., Helén, H., Roos, Y. H., and Jouppila, K. (2007). Effect of various polyols and polyol contents on physical and mechanical properties of potato starch-based films. *Carbohydr. Polym.* 67, 288–295. doi:10.1016/j.carbpol.2006.05.019
- Teodorescu, M., Bercea, M., and Morariu, S. (2019). Biomaterials of PVA and PVP in medical and pharmaceutical applications: perspectives and challenges. *Biotechnol. Adv.* 37, 109–131. doi:10.1016/j.biotechadv.2018.11.008
- Tsagkari, E., Connelly, S., Liu, Z., McBride, A., and Sloan, W. T. (2022). The role of shear dynamics in biofilm formation. *NPJ. Biofilms Microbiol.* 8, 33. doi:10.1038/s41522-022-00300-4

- Verma, N., Pramanik, K., Singh, A. K., and Biswas, A. (2022). Design of magnesium oxide nanoparticle incorporated carboxy methyl cellulose/poly vinyl alcohol composite film with novel composition for skin tissue engineering. *Mater. Technol.* 37, 706–716. doi:10.1080/10667857.2021.1873634
- Verma, R., Verma, S. K., Rakesh, K. P., Girish, Y. R., Ashrafzadeh, M., Sharath Kumar, K. S., et al. (2021). Pyrazole-based analogs as potential antibacterial agents against methicillin-resistance staphylococcus aureus (MRSA) and its SAR elucidation. *Eur. J. Med. Chem.* 212, 113134. doi:10.1016/j.ejmech.2020.113134
- Vishal Gupta, N., and Shivakumar, H. G. (2010). Preparation and characterization of superporous hydrogels as gastroretentive drug delivery system for rosiglitazone maleate. *Daru* 18, 200–210.
- Wiegand, I., Hilpert, K., and Hancock, R. E. W. (2008). Agar and broth dilution methods to determine the minimal inhibitory concentration (MIC) of antimicrobial substances. *Nat. Protoc.* 3, 163–175. doi:10.1038/nprot.2007.521
- Xia, Y., Yang, R., Wang, H., Li, Y., and Fu, C. (2022). Application of chitosan-based materials in surgical or postoperative hemostasis. *Front. Mater.* 9, 994265. doi:10.3389/fmats.2022.994265
- Yah, C. S., and Simate, G. S. (2015). Nanoparticles as potential new generation broad spectrum antimicrobial agents. *Daru J. Pharm. Sci.* 23, 43. doi:10.1186/s40199-015-0125-6
- Zhang, L., Yu, D., Regenstein, J. M., Xia, W., and Dong, J. (2021). A comprehensive review on natural bioactive films with controlled release characteristics and their applications in foods and pharmaceuticals. *Trends Food Sci. Technol.* 112, 690–707. doi:10.1016/j.tifs.2021.03.053
- Zhang, Y., Jiang, M., Zhang, Y., Cao, Q., Wang, X., Han, Y., et al. (2019). Novel lignin–chitosan–PVA composite hydrogel for wound dressing. *Mater. Sci. Eng. C* 104, 110002. doi:10.1016/j.msec.2019.110002
- Zou, S., Wang, B., Wang, C., Wang, Q., and Zhang, L. (2020). Cell membrane-coated nanoparticles: research advances. *Nanomedicine* 15, 625–641. doi:10.2217/nnm-2019-0388
- Zulhendri, F., Lesmana, R., Tandean, S., Christopher, A., Chandrasekaran, K., Irsyam, I., et al. (2022). Recent update on the anti-inflammatory activities of propolis. *Molecules* 27, 8473. doi:10.3390/molecules27238473